RESEARCH ARTICLE

Mapping Kainate Activation of Inner Neurons in the Rat Retina

Lisa Nivison-Smith,[1] Daniel Sun,[2,3] Erica L. Fletcher,[4] Robert E. Marc,[5] and Michael Kalloniatis[1,2,4,6]*

[1]School of Optometry and Vision Science, University of New South Wales, Sydney, New South Wales, 2052, Australia
[2]Department of Ophthalmology, Massachusetts Eye & Ear Infirmary, Boston, Massachusetts 02114
[3]Department of Optometry and Vision Science, University of Auckland, Auckland, 1142, New Zealand
[4]Department of Anatomy and Neuroscience, University of Melbourne, Parkville, 3010, Australia
[5]University of Utah School of Medicine, Department of Ophthalmology, University of Utah, Salt Lake City, Utah 84113
[6]Centre for Eye Health, Sydney, New South Wales, 2052, Australia

ABSTRACT

Kainate receptors mediate fast, excitatory synaptic transmission for a range of inner neurons in the mammalian retina. However, allocation of functional kainate receptors to known cell types and their sensitivity remains unresolved. Using the cation channel probe 1-amino-4-guanidobutane agmatine (AGB), we investigated kainate sensitivity of neurochemically identified cell populations within the structurally intact rat retina. Most inner retinal neuron populations responded to kainate in a concentration-dependent manner. OFF cone bipolar cells demonstrated the highest sensitivity of all inner neurons to kainate. Immunocytochemical localization of AGB and macromolecular markers confirmed that type 2 bipolar cells were part of this kainate-sensitive population. The majority of amacrine (ACs) and ganglion cells (GCs) showed kainate responses with different sensitivities between major neurochemical classes (γ-aminobutyric acid [GABA]/glycine ACs $>$ glycine ACs $>$ GABA ACs; glutamate [Glu]/weakly GABA GCs $>$ Glu GCs). Conventional and displaced cholinergic ACs were highly responsive to kainate, whereas dopaminergic ACs do not appear to express functional kainate receptors. These findings further contribute to our understanding of neuronal networks in complex multicellular tissues. J. Comp. Neurol. 521:2416–2438, 2013.

INDEXING TERMS: kainate; kainate receptors; agmatine; AGB; rat retina; glutamate; GABA; glycine; immunocytochemistry

In the retina, the effects of glutamate are mediated by ionotropic and metabotropic glutamate receptors. Ionotropic glutamate receptors are integral membrane proteins that form ligand-gated cation channels and mediate fast, excitatory synaptic transmission. They are classified as α-amino-3-hydroxy-5-methyl-isoxazole-4-propionic acid (AMPA), kainate (KA), and N-methyl-D-aspartate (NMDA) receptors based on pharmacological and electrophysiological characteristics (Monaghan et al., 1989; Seeburg, 1993; Hollmann and Heinemann, 1994). This study focuses on the KA-sensitive glutamate receptors—tetrameric proteins formed through combinations of five receptor subunits: glutamate (Glu)R5, GluR6, GluR7, KA1, KA2, and two orphan receptor subunits, δ1 and δ2 (Hollmann and Heinemann, 1994; Ozawa et al., 1998; Dingledine et al., 1999).

The expression of KA glutamate receptors was first demonstrated in the rodent retina by using in situ hybridization at the mRNA level. GluR5 is expressed in the outer half of the inner nuclear layer, suggesting its localization to bipolar cells (BCs) and horizontal cells (Hughes et al., 1992; Muller et al., 1992; Hamassaki-Britto et al., 1993). Some of these cell bodies also labeled for GluR6 and GluR7 (Hamassaki-Britto et al., 1993; Brandstätter et al., 1994). No labeling was seen for KA1 in the rodent retina, but many cell bodies labeled for KA2 (Brandstätter et al., 1994). Using subunit-specific immunocytochemical antibodies, processes of both amacrine cells (ACs) and ganglion cells (GCs) postsynaptic to cone BCs in both

Grant sponsor: the National Health and Medical Research Council of Australia; Grant numbers: 1009342 (to M.K. and E.L.F.) and 1021042 (to E.L.F. and M.K.); Grant sponsor: the National Institutes of Health; Grant numbers: EY02576 and EY014800 (to R.E.M.).

*CORRESPONDENCE TO: Michael Kalloniatis, Centre for Eye Health, University of New South Wales, Sydney, 2052, NSW, Australia.
E-mail: m.kalloniatis@unsw.edu.au

Received September 17, 2012; Revised December 6, 2012; Accepted January 17, 2013
DOI 10.1002/cne.23305
Published online January 24, 2013 in Wiley Online Library (wileyonlinelibrary.com)

sublaminae of the inner plexiform layer were shown to express various KA receptor subunits (Peng et al., 1995; Brandstätter et al., 1997; Qin and Pourcho, 2001). At the majority of these cone bipolar cell dyad contacts, immunoreactivity for the subunits was confined to only one of the postsynaptic elements, either an AC or a GC (Brandstätter et al., 1997; Qin and Pourcho, 2001). Postsynaptic to rod BCs, KA receptors are expressed on the AI ACs, but not the AII ACs (Ghosh et al., 2001). Whether these expressed subunits form functional KA receptors remains largely unknown.

Anatomical studies have identified AMPA and KA receptor subunits on OFF cone BCs postsynaptic to photoreceptors, but, as with other techniques, receptor functionality or identification of OFF BC type has not been determined (Brandstätter et al., 1997; Hack et al., 1999; Morigiwa and Vardi, 1999; Qin and Pourcho, 1999; Haverekamp et al., 2001). Electrophysiological studies demonstrate that morphologically distinct types of OFF BCs in the ground squirrel specifically express either AMPA- or KA-sensitive receptors (DeVries, 2000).

From this work arises an enduring issue in retinal physiology: to ascribe the locality of glutamate receptor subunits onto known cell types and determine their functionality. One approach for assessing glutamate receptor function is probing cation channel activation based on the entry of the organic cation 1-amino-4-guanidobutane (AGB). The immunocytochemical localization of accumulated AGB in retinal sections provides a map of neuronal activity with high spatial resolution. The AGB technique also preserves structural integrity of the retina, thus allowing for cellular identity. The mechanisms of AGB permeation and its advantages in studying neuronal networks have been expounded in multiple studies (Marc, 1999a,b; Marc and Jones, 2002; Sun et al., 2003; Kalloniatis et al., 2004; Marc et al., 2005; Sun and Kalloniatis, 2006). In the mouse retina, CD15-immunoreactive BCs were AGB permeable secondary to AMPA activation, but not KA activation, demonstrating that this cation can be used to investigate glutamate receptor functionality in neurochemically identified populations (Sun and Kalloniatis, 2006).

In this study, we describe the KA sensitivity of different neurochemically identified inner retinal neurons within an intact retinal network. We segregated neurons into separate classes by quantitative immunocytochemistry of the amino acids glutamate (Glu), γ-aminobutyric acid (GABA), and glycine (Gly) and determined the KA sensitivity of these populations by overlapping AGB permeation with amino acid profiles (Marc et al., 1990, 1995, 2005; Kalloniatis et al., 1996; Marc, 1999a,b; Marc and Jones, 2002; Sun et al., 2003). We then used indirect immunofluorescence to detect AGB to assigned KA receptor functionality to specific cell classes based on macromolecular markers (Sun and Kalloniatis, 2006; Sun et al., 2007a,c). We show that various retinal neuron populations (i.e., BCs, ACs, GCs) are activated by KA. The combination of macromolecular markers and amino acid immunocytochemistry can be used to assign KA receptor functionality to specific subpopulations, e.g., functional activation of the cholinergic AC population, a subgroup of the GABA AC population (Sun et al., 2007a–c). We also highlight the need for careful interpretation of AGB labeling when using broad-acting glutamate receptor agonists.

MATERIALS AND METHODS

Retinal preparation and incubation

Adult male Sprague-Dawley rats ($n = 30$) obtained from Animal Resources Centre (Canning Vale, WA, Australia) were deeply anesthetized with an intramuscular injection of ketamine (100 mg/kg; Phoenix Pharm, Auckland, New Zealand) and domitor (1 mg/kg; Novartis Animal Health, Melbourne, Australia) and following the retinal dissection, were killed with an intracardial injection of potassium chloride. Isolated retinal samples were mounted on 0.8 μm pore Metricel membrane filters (Gelman Sciences, Ann Arbor, MI), and the retinal pigment epithelium was separated from the retina by gently pulling the globe away from the filter paper. Retinal pieces were incubated in vitro in a modified Edwards medium (Edwards et al., 1989) to which 25 mM AGB was added and an equimolar reduction in NaCl concentration was made. For the activation studies, various concentrations of KA (1–80 μM) were added to the incubation medium. All incubations were performed under normal room lighting (300–400 lux) for 6 minutes at 37°C with the medium bubbled in 95% O_2/5% CO_2. The experimental protocols in this study were approved by The University of Auckland and The University of New South Wales animal ethics committee.

Postembedding immunocytochemistry

The procedures for postembedding immunocytochemistry have been described previously (Marc et al., 1990, 1995; Kalloniatis and Fletcher, 1993; Sun et al., 2003). Briefly, retinal pieces were fixed in 2.5% (w/v) glutaraldehyde, 1% (w/v) paraformaldehyde in 0.1 M phosphate buffer (PB) at pH 7.4 for 30 minutes, washed in PB, and dehydrated through cold methanol to acetone before impregnating in resin. Resin blocks were sectioned at 250 nm to allow subsequent serial sectioning for postembedding immunocytochemistry (Sun et al., 2003). Primary antibodies were diluted in 1% goat serum in phosphate-buffered saline to the concentrations specified in Table 1. The primary antibodies were detected with goat

TABLE 1.
Antibodies Used in This Study

Antigen	Immunogen	Manufacturer, cat. no.	Host	Dilution
Agmatine (AGB)	Agmatine conjugated to bovine serum albumin	Chemicon (Millipore); AB1568[1]	Rb; polyclonal	1:100 (IF); 1:800 (ICC)
Agmatine (AGB)	Agmatine cross-linked to purified fraction V bovine serum albumin with glutaraldehyde	Abcam; ab62667[1]	Ch; polyclonal	1:500
Calretinin	Recombinant rat calretinin	Millipore; MAB1568	Ms; monoclonal	1:1,000
Choline acetyl transferase (ChAT)	Highly purified ChAT obtained from porcine brain	Chemicon (Millipore); MAB5270	Ms; monoclonal	1:500
γ-Aminobutyric acid (GABA)	GABA conjugated to bovine serum albumin with glutaraldehyde	Chemicon (Millipore); AB5016[1]	Rb; polyclonal	1:4,500
Glutamate	Glutamate conjugated to bovine serum albumin with glutaraldehyde	Chemicon (Millipore); AB5018[1]	Rb; polyclonal	1:4,500
Glycine	Glycine conjugated to bovine serum albumin with glutaraldehyde	Chemicon (Millipore); AB5020[1]	Rb; polyclonal	1:4,000
Islet-1	Truncated rat islet protein corresponding to amino acids 178–349	Developmental Studies Hybridoma Bank; 39.4D5	Ms; monoclonal	1:200
Neurokinin receptor 3 (NK3R)	Synthetic peptide (SSFISSPYTSSVDEYS) corresponding to amino acids 451–465 of rat NK-3 conjugated to bovine thyroglobulin	Novus Biologicals; NB300-102	Rb; polyclonal	1:4,000
Nitric oxide synthase-brain (bNOS)	Recombinant neuronal NOS fragment (amino acids 1–181) from rat brain	Sigma-Aldrich; N2280	Ms; monoclonal	1:3,000
Parvalbumin (PV)	Frog muscle parvalbumin	Sigma-Aldrich; P3088	Ms; monoclonal	1:500
Protein kinase C-α (PKCα)	Purified bovine brain PKC	Sigma-Aldrich; P5704	Ms; monoclonal	1:400
Protein kinase C-α (PKCα)	Synthetic peptide (KVNPQFVHPILQSAV) corresponding to amino acids 659–672 from the C-terminal variable region of rat PKCα	Sigma-Aldrich; P4334	Rb; monoclonal	1:2,000
Recoverin	Recombinant human recoverin	Chemicon (Millipore); AB5585	Rb; polyclonal	1:1,000
Tyrosine hydroxylase (TH)	Denatured tyrosine hydroxylase from rat pheochromocytoma (denatured by sodium dodecyl sulfate)	Chemicon (Millipore); AB152	Rb; polyclonal	1:1,000

[1]These antibodies were kindly donated by Dr. R.E. Marc, are licensed to Signature Immunologics, and are also commercially available through Abcam and/or Merck Millipore. Abbreviations: Rb, rabbit; Ch, chicken; Ms, mouse, IF, immunofluorescence, ICC, immunocytochemistry.

anti-rabbit secondary antibodies (British BioCell, Cardiff, UK) coated with a 1-nm gold particle at a dilution of 1:100. The immunogold was visualized by silver intensification (Marc et al., 1990; Kalloniatis and Fletcher, 1993; Sun et al., 2003).

Indirect immunofluorescence

Retinal pieces were fixed in 4% (w/v) paraformaldehyde, 1% (w/v) glutaraldehyde in PB for 30–40 minutes. The samples were cryoprotected in a graded sucrose solution (10–30%) overnight and then mounted in freezing medium (Reichert, Nussloch, Germany). Vertical sections at 16 μm thickness were collected on positively charged slides (Lomb Scientific, Taren Point, Australia).

The indirect immunofluorescence technique was performed as outlined in Sun and Kalloniatis (2006). Antisera were diluted in PB containing 3% goat serum, 1% bovine serum albumin, and 0.5% (v/v) Triton X-100. Descriptions of the antibodies used and their concentrations are

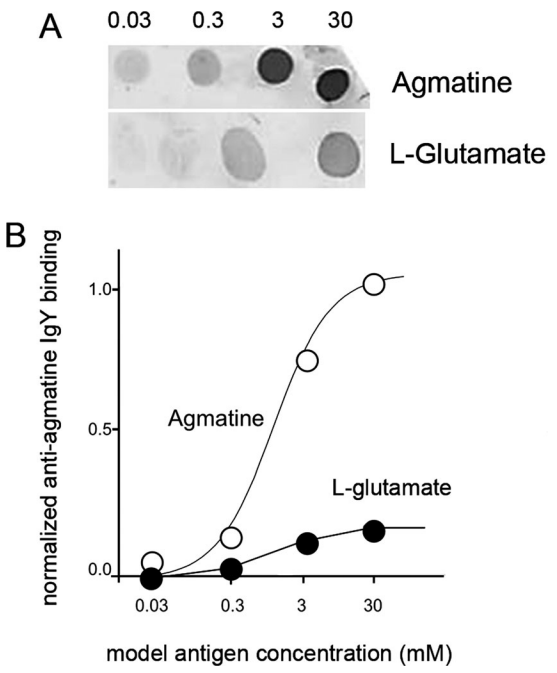

Figure 1. Characterization of the chicken anti-AGB antibody. **A:** Dot blots show anti-agmatine binding to purified ovalbumin–glutaraldehyde–agmatine and ovalbumin–glutaraldehyde–glutamate conjugates. **B:** Density measures were converted to linear binding intensity, plotted against first-order binding curves (white circles, AGB; black circles, glutamate).

presented in Table 1. Sections were initially incubated in PB containing 6% goat serum, 1% bovine serum albumin, and 0.5% (v/v) Triton X-100 for 1 hour at room temperature followed by incubations with primary antibodies overnight at 4°C. The secondary antibodies were conjugated to Alexa Fluor 405, Alexa Fluor 488, or Alexa Fluor 594 (Molecular Probes, Eugene, OR). The specificity of the secondary antibodies was confirmed by omitting the primary antibody or using a secondary antibody from a different species.

All the immunofluorescent micrographs were collected by using a confocal laser scanning microscope (LEICA Microsystems TCS 4D). The brightness and contrast of the final images were adjusted by using Adobe Photoshop (version 6; Adobe Systems, Mountain View, CA). Quantification of AGB-labeled cells was performed as previously described (Acosta et al., 2007; Sun and Kalloniatis, 2006). Briefly, cells with distinctly AGB labeled somata from background levels were counted as KA-activated cells and were noted to be colocalized if there was overlapping marker immunoreactivity at the same anatomical location. Areas showing obvious anatomical disruptions were excluded. Data are presented as the mean ± standard deviation of five independent retinae, and statistical significance was determined by using a one-way analysis of variance (ANOVA) across three KA concentrations (5, 20, and 80 μM).

Antibody characterization

Amino acids (GABA, glutamate, and glycine)

The specificity of the amino acid antibodies has been demonstrated in dot immunoassays. A positive signal for the GABA antibody was obtained for an artificial GABA antigen coupled to bovine serum albumin via glutaraldehyde cross-linking (Marc et al., 1990, 1995). Identical results were seen for glutamate and glycine antibodies with glutaraldehyde cross-linked glutamate and glycine antigens. No cross-reactivity was observed with amino acids other than that of the antibody target (manufacturer's data sheet, Marc et al., 1990, 1995).

AGB

The specificity of the AGB antibody hosted in rabbit has been previously confirmed with dot blot immunoassays, which report no cross-reactivity with other amino acids (Marc, 1999b). For anti-agmatine IgY hosted in chicken, the immunogen was purified agmatine attached to terminal amino groups on a proprietary carrier peptide via an N-linked pentane spacer. The resulting chicken IgY was purified by using serial polyethylene glycol and octanol precipitations. The specificity was first assayed on previously agmatine-loaded tissue samples and found to be indistinguishable from the anti-agmatine IgG labeling published by Marc (1999b). Specificity and cross-reactivity with other potential targets was tested with pattern recognition (Marc et al., 1995), competition assays (Jones et al., 2011), and dot blots (Marc et al., 1990). Figure 1 shows a dot blot of anti-agmatine IgY binding to purified ovalbumin–glutaraldehyde–agmatine and ovalbumin–glutaraldehyde–glutamate conjugates. Glutamate was chosen as it showed the most cross-reactivity of the entire amino acid set against which anti-agmatine IgY was tested. The density measures were converted to linear binding intensity, plotted against first-order binding curves. These results are similar to other previously reported anti-amino binding selectivities. The implication is that any cell with an agmatine content of ≈3 mM (a very large signal) could have a maximum possible contamination of that signal by endogenous glutamate of ≈10% if the cell also contained 3–30 mM glutamate. Cells with less glutamate will generate a pure agmatine signal.

Calretinin

The specificity of the calretinin antibody was confirmed in western blots of mouse brain lysate, in which it presented as a single 31-kDa band (manufacturer's data sheet).

Choline acetyl transferase (ChAT)

The specificity of the ChAT antibody was observed in western blots using purified ChAT from porcine brain, where it yielded an immunoreactive band of 67 -kDa (Ostermann-Latif et al., 1992).

Islet-1

The specificity of Islet-1 antibody was confirmed in immunostaining that showed Islet-1 immunoreactivity in Chinese hamster ovary (CHO) cells transfected with Islet-1 expression vector but not in normal CHO cells (Thor et al., 1991).

Neurokinin receptor 3 (NK3R)

Specificity of NK3R antibody has been previously demonstrated by immunohistochemical staining in rat brain and preadsorption studies with NK-3 peptide in which the signal was completely abolished by the peptide (manufacturer's data sheet, personal communication with manufacturer). Labeling patterns observed in this study also matched NK3R immunoreactivity demonstrated in the rat retina by using a separate NK3R antibody developed from a synthetic peptide (SSRKKR) corresponding to amino acids 410–417 of rat NK3 (Casini et al., 2000; Grady et al., 1996).

Brain nitric oxide synthase (bNOS)

bNOS antisera specificity was shown previously in western blots in which the antibody reacted with NOS from rat cerebellum at the expected molecular weight (155 -kDa) and not with NOS from macrophages or endothelial cells (manufacturer's data sheet; Dinerman et al., 1994).

Parvalbumin (PV)

The specificity of antibody for PV has been previously shown in western blots of rat brain and muscle extracts in which the antibody recognizes a 12-kDa protein corresponding to PV (Heizmann and Celio, 1987).

Protein kinase C-α (PKCα)

The specificity of the monoclonal PKCα antibody raised in mouse was confirmed in a western blot of rat glioma extract and NIH 3T3 mouse fibroblast lysate in which the antibody reacted with a single 80-kDa band corresponding to the expected size for PKCα (Young et al., 1988). The specificity of the polyclonal PKCα antibody raised in rabbit was confirmed in western blots using rat brain extracts and NIH 3T3 cell lysate as the presence of an 80-kDa band (manufacturer's data sheet).

Recoverin

Specificity of this antibody was confirmed in western blots of human adult retina tissue homogenate as the presence of single 26-kDa band (Yan and Wiechmann, 1997).

Tyrosine hydroxylase (TH)

The specificity of the antibody for TH has been demonstrated by labeling of a single 62-kDa band in western blots of brain tissue lysate (Haycock, 1987).

Neuron classification by amino acid labeling patterns

Neurons were classified based on the differential localization of amino acids as described previously (Pourcho, 1980; Marc et al., 1990, 1995, 2005; Davanger et al., 1991; Crooks and Kolb, 1992; Kalloniatis et al., 1996; Marc, 1999a,b; Pow, 2001; Marc and Jones, 2002; Sun et al., 2003). Serial semithin sections from identical retina locations were labeled for Glu, GABA, and Gly, and the cells were segregated into the following categories: BCs (OFF cone BCs, i.e., Gly negative), ACs (GABA only, Gly only, and GABA/Gly), GCs (Glu, Glu/weakly GABA), and displaced ACs. The small cell bodies, location, and intense GABA staining of displaced ACs allowed them to be separated from GCs (Yu et al., 1988; Kalloniatis et al., 1996; Marc and Jones, 2002). This broad categorization does not allow for the multitude of amino acid classes that can arise from pattern recognition analysis (Marc et al., 1995; Kalloniatis et al., 1996; Marc and Jones, 2002); however, it is less time consuming and allows for a larger sample size appropriate for cell counts and dose–response functions.

Dose–response curves

For each KA concentration, samples were obtained from four independent retinae. Cells were classified as being immunoreactive for AGB, Glu, GABA, Gly, or a combination thereof. For each neurochemical population, two dose–response functions were generated. The first (Figs. 3, 10, and 12, black lines) represents the percentage of cells activated as a proportion of the total number of BCs, ACs, or GCs. This function answers the question: Of the total number of activated ACs, what percentages were GABA- or Gly-immunoreactive ACs? The second function (Figs. 3, 10, and 12, gray lines) represents the percentage of cells activated as a proportion of the total number of cells belonging to that neurochemical class. This function answers the question: Of all the GABA-immunoreactive ACs, what percentages are activated at the various KA concentrations, and what final percentages are activated at saturating levels? At a saturating level of KA (80 μM), it was difficult to identify the displaced ACs and therefore, both response functions for this population were modeled on only five datum points (Fig. 12D). Procedures for the cell counting and the criterion chosen for considering a cell as being labeled have been described previously (Sun et al., 2003). Response curves were fitted by using a Naka–Rushton equation:

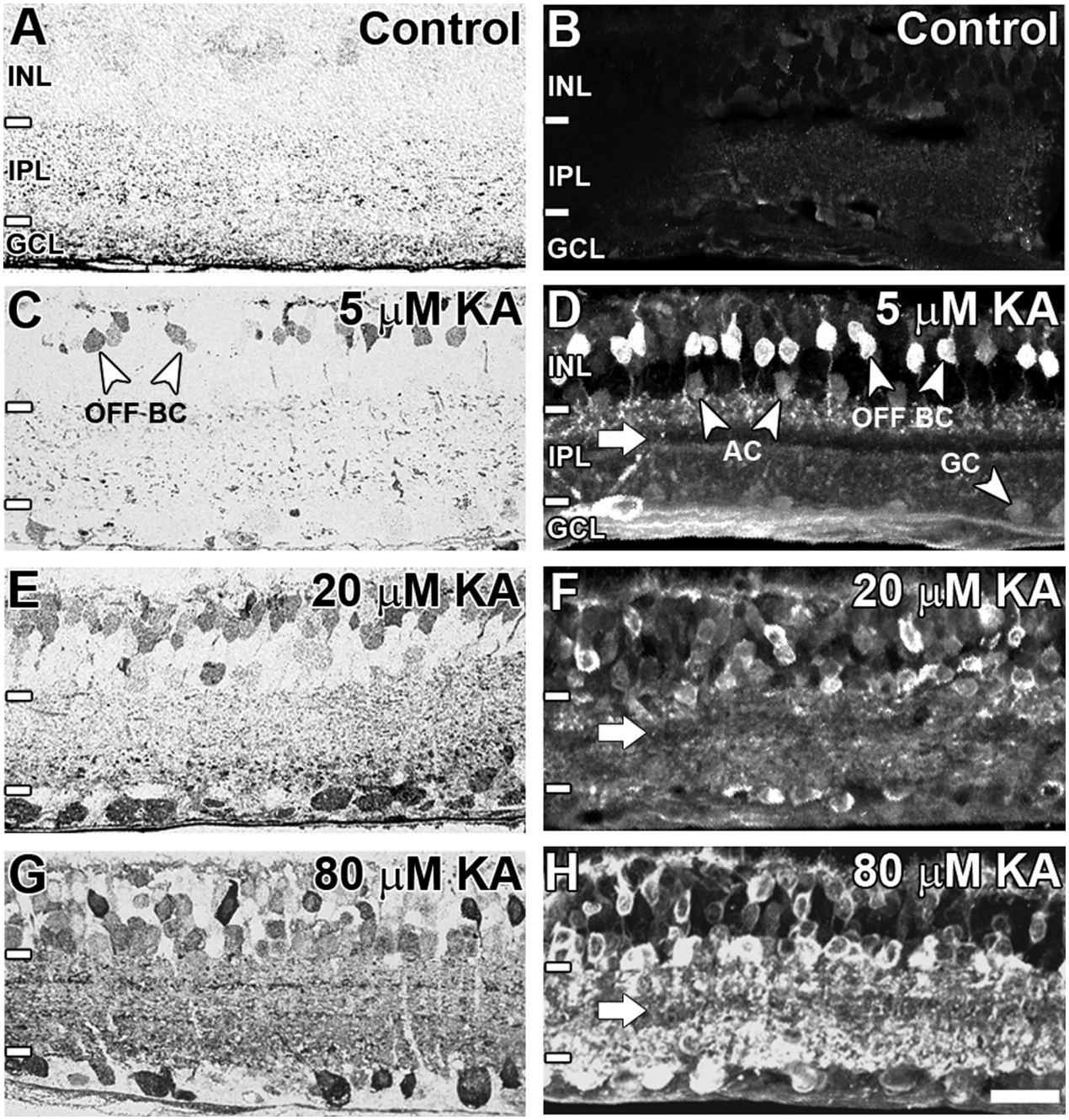

Figure 2. AGB immunoreactivity in the adult rat retina at (**A,B**) basal levels, (**C,D**) 5 μM kainate (KA) activation, (**E,F**) 20 μM KA activation, and (**G,H**) 80 μM KA activation. Sections were imaged with brightfield light microscopy using postembedding immunocytochemistry (A,C,E,G) or confocal microscopy using indirect immunofluorescence (B,D,F,H). Retinal layers including the inner nuclear layer (INL), inner plexiform layer (IPL), and ganglion cell layer (GCL) are indicated by white lines and annotations on the left-hand side of the image. The white arrow indicates weakly AGB-immunoreactive strata in the IPL. BC, bipolar cell; AC, amacrine cell; GC, ganglion cell. Scale bar = 20 μm in H (applies to A–H).

$$\frac{R}{R_{max}} = \frac{C_{KA}^n}{C_{KA}^n + K^n}$$

where R is the response, R_{max} is the maximum labeling response, C_{KA} is the KA concentration, n is the slope parameter, and K is the KA concentration for a half-maximal response.

A nonparametric bootstrap algorithm was used to assess the reliability of the data. This method does not rely on any underlying assumptions about the data and is useful when the sample size is small (Efron and Tibshirani, 1986; Foster and Bischof, 1987; Bui et al., 1998, 2005). Each iterative bootstrap sample consisted of *n* random

selections taken (with replacement) from the available data in each KA concentration group. A pseudo-replication of the dataset is obtained, and each dataset is fitted to obtain estimates of the data descriptive parameters. The bootstrap method allows error estimates to be obtained from the parameters of a fitted function. Although the distribution of the true dataset is not known, the estimate obtained by the resampling strategy provides an approximation of the empirical distribution (Darvas et al., 2004). We applied this bootstrap technique to the dataset of the percentage of activated cells as a function of KA concentration and obtained estimates of the R_{max}, n, and K. The mean parameter value and 95% confidence interval (the 2.5th and 97.5th percentiles were taken as the bounds) for each of the parameters were obtained after 1,000 bootstrap repetitions. We considered two population parameters as significantly different when the mean parameter of population *a* does not lie within the confidence interval of population *b*. In this case, we are determining whether the means of a parameter for the two populations are significantly different from each other, but not necessarily separable because 2.5% of the parameter probability distribution function may overlap.

RESULTS

KA-induced AGB permeation

AGB labeling secondary to KA activation was visualized by using postembedding immunocytochemistry (Fig. 2A,C,E,G) and indirect immunofluorescence (Fig. 2B,D,F,H). Short-term incubations of isolated retina in medium containing AGB led to no significant neuronal labeling (Fig. 2A,B). This is consistent with there being no measurable endogenous AGB signal in the retina (Marc, 1999b; Kalloniatis et al., 2002; Sun and Kalloniatis, 2006). The addition of KA resulted in a dose-dependent AGB entry confined to the inner retina (Fig. 2C–H). Application of 5 μM KA preferentially activated subpopulations of OFF cone BCs (Fig. 2C,D). In Figure 2D, the axon terminals of these BCs can be seen terminating in sublamina *a* (or the OFF sublamina) of the inner plexiform layer. Light labeling of some ACs and GCs was also evident. Increasing concentrations of KA led to a greater number of AGB-labeled cells throughout the inner nuclear and ganglion cell layers (20 μM: Fig. 2E,F; 80 μM: Fig. 2G,H). This was reflected in the increasingly dense punctate staining within the inner plexiform layer. One strata of the inner plexiform layer displayed weak background AGB labeling, most obvious at 5 μM KA and still evident at 80 μM KA (Fig. 2D,F,H; white arrows).

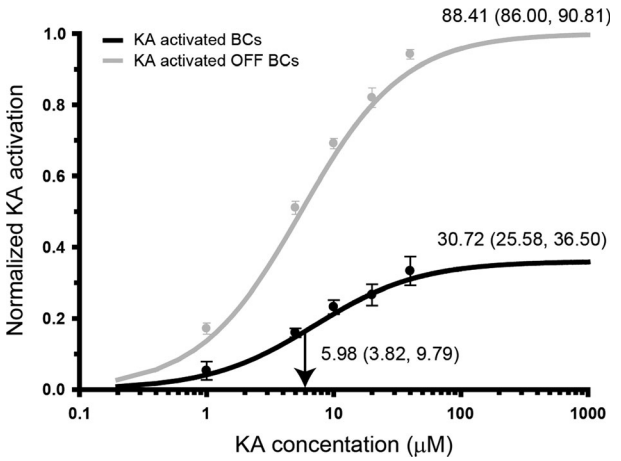

Figure 3. KA dose–response curves for OFF cone and total bipolar cell (BC) populations. The black line indicates the number of kainate (KA)-activated BCs in the cell population as a percentage of the total number of BCs present ($n = 556$). The gray line indicates the percentage of OFF BCs activated by KA. KA concentration is presented as a log 10 scale on the x-axis; percentage activation on the y-axis is presented as a normalized response where 1.0 indicates activation of 100% of the population. Annotations at the activation curve plateau indicate the mean total percentage of cells activated at saturating KA concentrations (80 μM KA). Vertical black arrows and their annotations delineate the half-maximal KA concentration. Bracketed values indicate the bounds of the 95% confidence interval. The data points in the dose–response curve have had the proportion of basal AGB-labeled cells subtracted so each datum point reflects true KA activation.

Characterization of KA-activated BC populations

Response of OFF BCs to KA

Dose–response curves for KA activation of inner retinal neurons were generated from serial semithin sections labeled for AGB, glutamate, GABA, and glycine. BCs were segregated into ON cone BCs (identified by Gly immunoreactivity), rod BCs (identified by high basal AGB labeling localized to cell somata and dendritic terminals), and OFF cone BCs (Sun et al., 2007a,c). BC activation showed a dose-dependent relationship with KA (Fig. 3). At saturating levels (80 μM KA), 30.7% of all BCs were activated. This population presumably consisted mostly of OFF cone BCs, as 88.4% of OFF cone BCs exhibiting functional glutamate receptors were responsive to KA. The half-maximal concentration for BCs (5.98 μM KA) was significantly less than other inner retinal neurons (see Figs. 10 and 12). This was consistent with previous observations that BCs were strongly labeled at lower KA concentrations compared to ACs and GCs (Marc, 1999b; Sun and Kalloniatis, 2006).

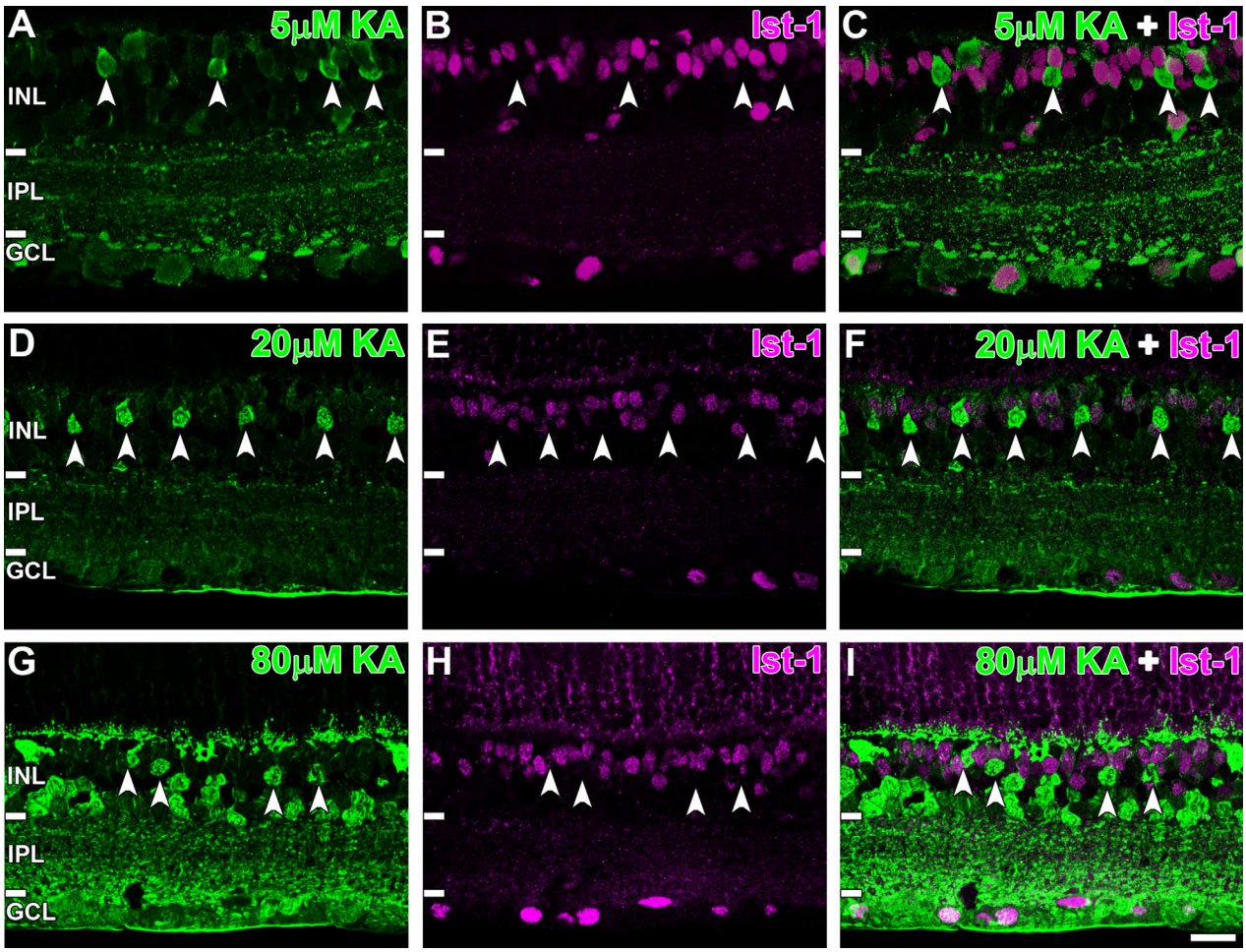

Figure 4. Confocal micrographs of AGB (green) and Islet-1 (Ist-1; magenta) immunoreactivity after activation with (**A–C**) 5 μM, (**D–F**) 20 μM, and (**G–I**) 80 μM kainate (KA). Activated bipolar cells (BCs; white arrowheads) did not colocalize with the Islet-1–positive-somata at any KA concentration used. Retinal layer annotations are the same as in Figure 2. Scale bar = 20 μm in I (applies to A–I).

Identification of activated OFF BC types with macromolecular markers

KA-activated BCs were further studied by colocalizing AGB with macromolecular markers. ON cone and rod BCs, identified by Islet-1 immunoreactivity, rarely colocalized with AGB at all KA concentrations (Fig. 4, white arrowheads). This was confirmed with cell counts showing that only 1.6 ± 1.2% of Islet-1 positive BCs colocalized with AGB at 80 μM KA (see Fig. 8A), corresponding to basal values observed in nonactivated mouse retinae (Sun and Kalloniatis, 2006).

Rod BCs, identified by PKCα labeling (Greferath et al., 1990) also showed very low colocalization with AGB-positive BCs at all KA concentrations used (Fig. 5, white arrowheads). In addition, a clear contrast could be seen in the location of the axon terminals of KA-activated BCs (in sublamina *a*) compared to PKCα-immunoreactive BC axons terminating in sublamina *b* (Fig. 5C, black and white arrow respectively). Cell counts indicated that only 2.7 ± 1.0% of PKCα immunoreactive BCs were activated at saturation levels (see Fig. 8A), matching basal colocalization levels (Sun and Kalloniatis, 2006). These results indicate that rod and ON cone BCs do not express functional KA-sensitive glutamate receptors in the rat retina.

OFF cone BCs were further segregated with the signaling molecule NK3R and the calcium binding protein recoverin (Figs. 6, 7). Previous work suggests that NK3R labels type 1 and type 2 OFF cone BCs in the rat retina (Oyamada et al., 1999; Casini et al., 2000; Haverkamp et al., 2003; Ghosh et al., 2004). The activation of NK3R-immunoreactive BCs by KA is shown in Figure 6. Faint NK3R immunoreactivity was present in sublamina *a* (Fig. 6B, white arrow) but not sublamina *b*, which is consistent with NK3R-immunoreactive cells being part of the OFF cone BC class. At all KA concentrations, AGB and NK3R colocalized in many BCs (Fig. 6, white arrowheads) but not all, indicating that only some NK3R BCs displayed functional glutamate receptors responsive to KA. This

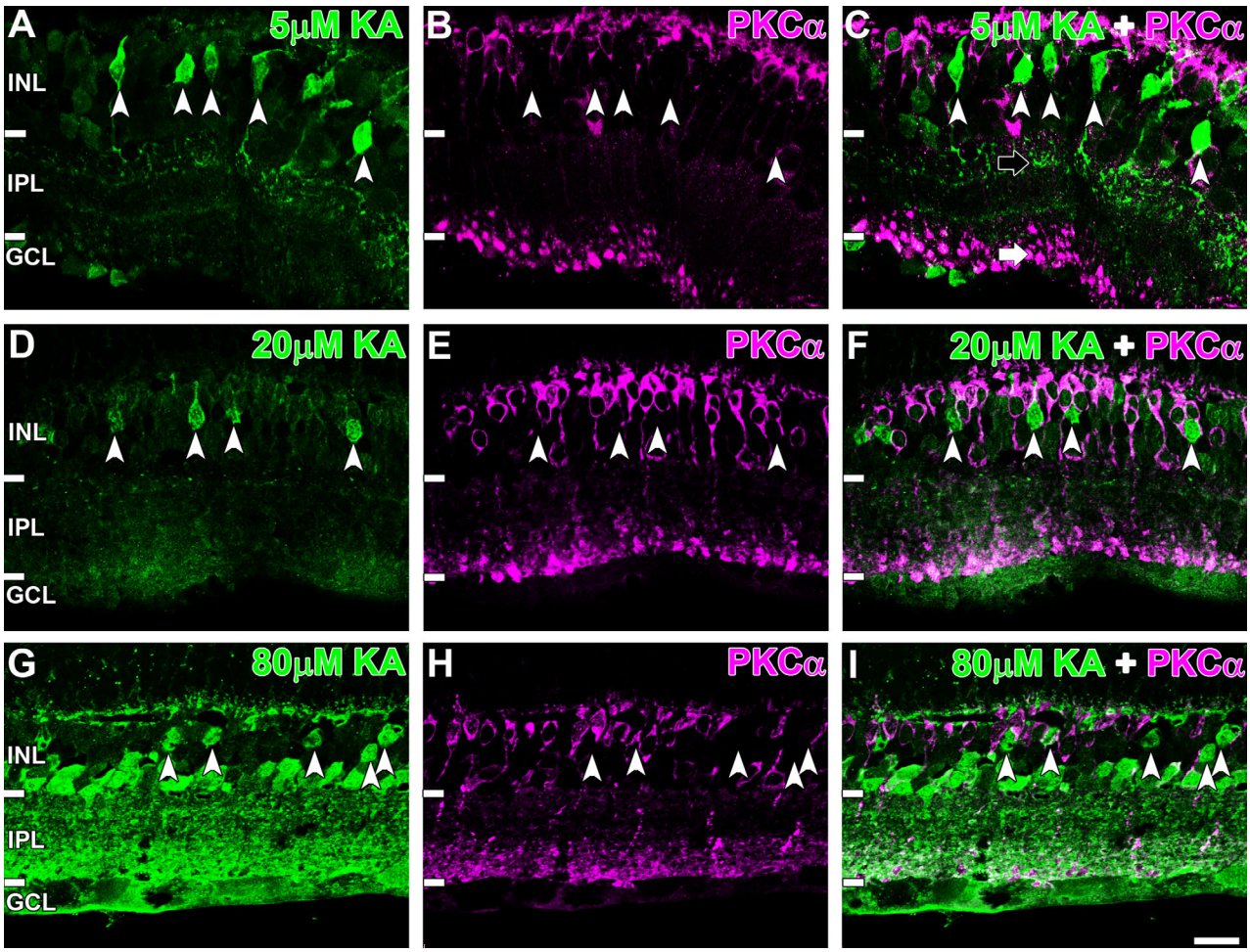

Figure 5. Immunoreactivity of AGB (green) and the rod bipolar cell (BC) marker protein kinase C-α (PKCα; magenta) secondary to (**A–C**) 5 μM, (**D–F**) 20 μM, and (**G–I**) 80 μM kainate (KA) activation. PKCα did not colocalize with activated BCs (white arrowheads) at all KA concentrations shown. PKCα-immunoreactive axon terminals localized to sublamina *b* are indicated by the white arrow, and the KA-activated terminals are indicated by the black arrow. Retinal layer annotations are the same as in Figure 2. Scale bar = 20 μm in I (applies to A–I).

was supported by quantitative analysis, which found that 56 ± 6.4% of NK3R-immunoreactive cells were activated at 80 μM KA (Fig. 8A). Colocalization values below saturation point (5 μM: 59 ± 11%, 20 μM: 57 ± 11%) were not significantly different from saturating KA levels (one-way ANOVA, $P = 0.90$), suggesting that maximum activation of KA-sensitive NK3R BCs occurs at low KA concentrations.

Recoverin labels type 2 OFF cone BCs as well as type 8 ON cone BCs and photoreceptors in the rat retina (Euler and Wässle, 1995; Milam et al., 1993). Consistent with this, we observed recoverin-immunoreactive axons in sublamina *a* and sublamina *b*, indicating the labeling of OFF and ON BC populations, respectively (Fig. 7B, white arrows). At low activation conditions, some recoverin BCs were activated (Fig. 7A–C, white arrowheads), but many were not activated (Fig. 7A–C, black arrowheads). This activation increased at 20 μM KA (Fig. 7D–F) and 80 μM KA (Fig. 7G–I). Quantification of activation showed that 42 ± 7.0%, 48 ± 8.5%, and 56 ± 12% of recoverin-immunoreactive BCs were activated at 5 μM, 20 μM, and 80 μM KA, respectively (Fig. 8A). A significant increase in colocalization occurred with increasing KA, suggesting dose-dependent activation of recoverin-immunoreactive cells by KA (one-way ANOVA, $P = 0.044$).

Recoverin-immunoreactive BCs were separated into type 2 and type 8 BCs with the ON cone and rod BC marker Islet-1 (Fig. 9). Type 2 BCs were identified as recoverin positive, Islet-1 negative (Fig. 9C–E, white arrowheads), and type 8 BCs were identified as recoverin and Islet-1 positive (Fig. 9C–E, black arrowheads). Colocalization with AGB confirmed that activated recoverin-labeled BCs were exclusively type 2 (Fig. 9F, white arrowheads) and not type 8 (Fig. 9F, black arrowheads). Quantification at saturating KA levels showed that 45 ± 4.3% of type 2 BCs were activated, but only 2.7 ± 0.7%

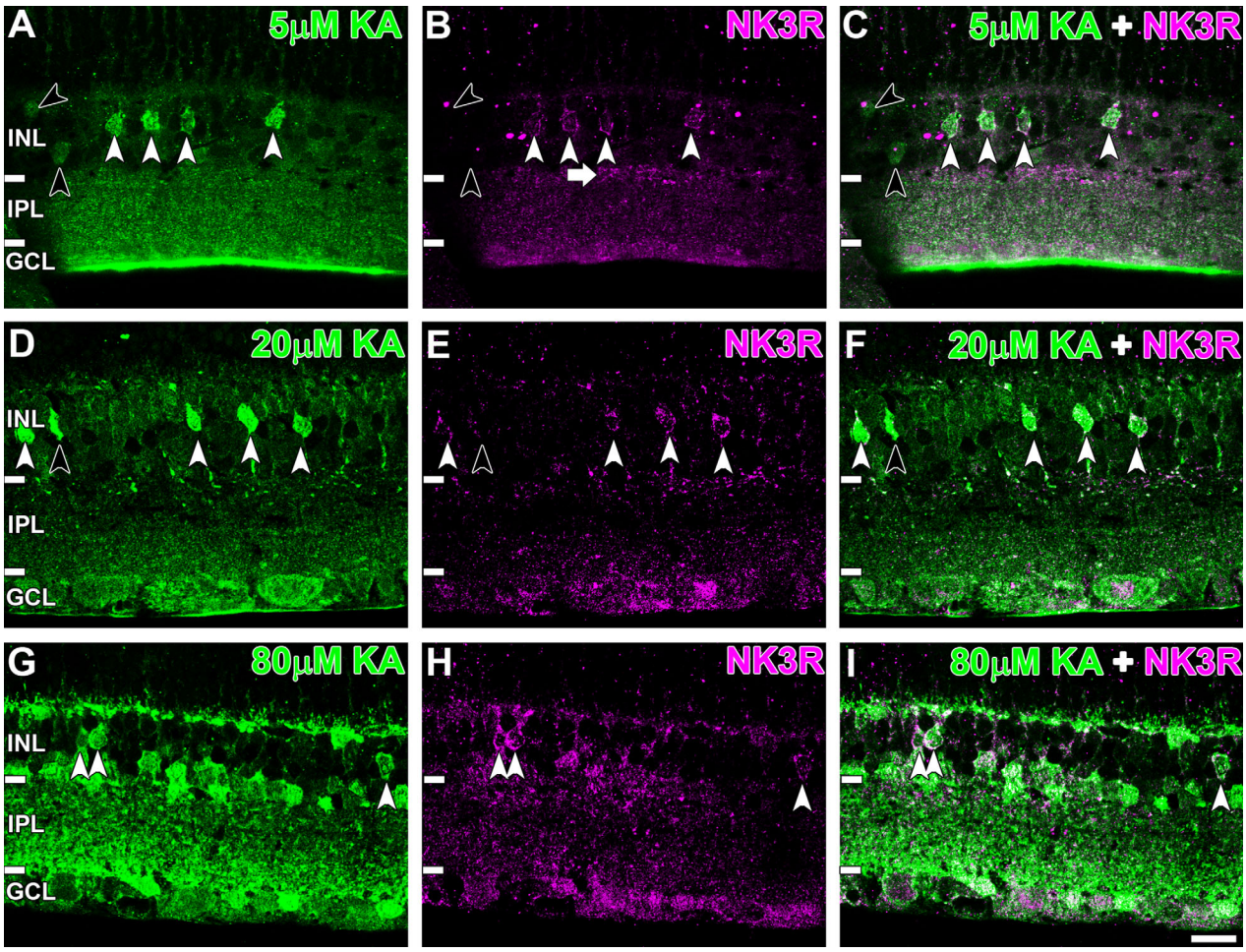

Figure 6. AGB (green) and neurokinin 3 receptor (NK3R; magenta) immunoreactivity after activation with (**A–C**) 5 μM, (**D–F**) 20 μM, and (**G–I**) 80 μM kainate (KA). At all activation concentrations, colocalization of some NK3R and KA-activated bipolar cells (BCs) was observed (white arrowheads). Some activated BCs were not immunoreactive for NK3R (black arrowheads). NK3R-immunoreactive BCs that were not activated by KA are marked with a black arrow. NK3R-immunoreactive axon terminals were exclusively localized to sublamina *a*, as indicated by the white arrow. Retinal layer annotations are the same as in Figure 2. Scale bar = 20 μm in I (applies to A–I).

type 8 BCs were activated (Fig. 9G). There was no significant difference between the number of activated recoverin cells in Figure 8A and the number of activated type 2 cells in Figure 9G (Student's *t*-test, $P = 0.11$).

The remaining OFF cone BC types (type 3 and 4) were analyzed as activated BCs that did not colocalize with recoverin or NK3R (Fig. 8B). Between 5 μM and 80 μM KA, the number of activated recoverin-negative (types 1, 3, and 4 BCs) and NK3R-negative (types 3 and 4 BCs) cells increased, consistent with dose activation curves (Fig. 3). This increase, however, did not reach significance (one-way ANOVA, Rec negative: $P = 0.12$, NK3R negative: $P = 0.85$). There was also no significant difference between the total number of activated recoverin-negative cells (28 ± 5.0%) and activated NK3R-negative BCs (40 ± 13%) at saturation point (Student's *t*-test, $P = 0.11$).

Characterization of KA-activated AC populations

Response of major neurochemical classes of ACs to KA

ACs were segregated according to their major neurochemical groupings: GABA-immunoreactive ACs, glycine-immunoreactive ACs, and GABA/glycine-immunoreactive ACs. A summary of activation characteristics of each cell class is shown in Table 2. For all populations, activation proceeded in a dose-dependent manner. At 80 μM KA, 86.3% of all ACs were activated, suggesting that most ACs express functional glutamate receptors responsive to KA (Fig. 10A). The half-maximal concentration for ACs was 30.0 μM KA.

GABA-immunoreactive ACs represented a significantly larger population (Fig. 10B; 46.2%) compared to the glycine-immunoreactive ACs (Fig. 10C; 36.7%). At saturation,

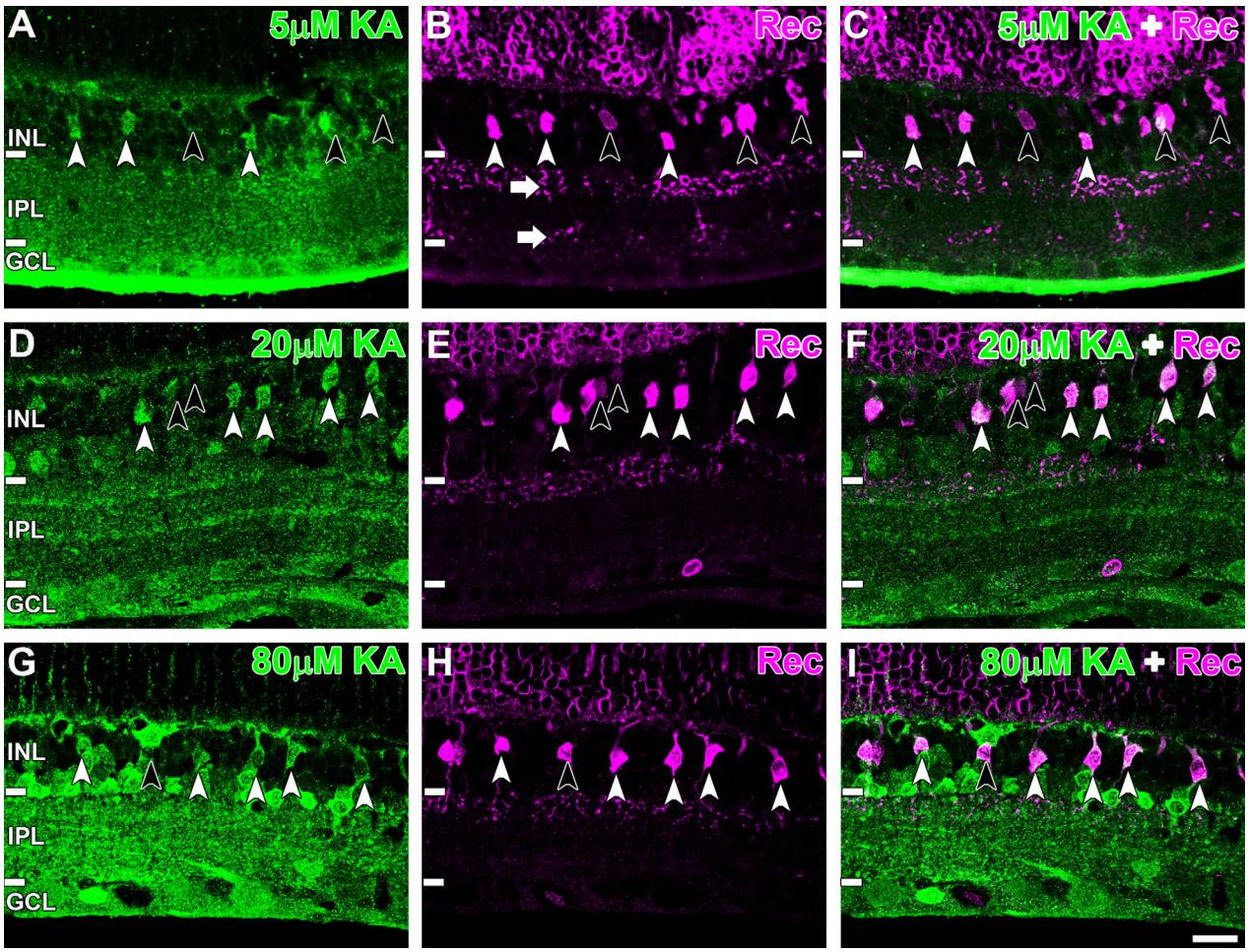

Figure 7. AGB (green) and recoverin (Rec; magenta) immunoreactivity after activation with (**A–C**) 5 μM, (**D–F**) 20 μM, and (**G–I**) 80 μM kainate (KA). White arrowheads indicate recoverin-immunoreactive bipolar cells (BCs) activated by KA, and black arrowheads indicate recoverin BCs that were not activated. White arrows indicate the recoverin-positive axon terminals in sublamina *a* and *b*. Retinal layer annotations are the same as in Figure 2. Scale bar = 20 μm in I (applies to A–I).

86.3% of GABA-immunoreactive ACs responded to KA, which was not significantly different from the glycine-immunoreactive AC population (85.6%). Comparison of the half-maximal KA concentration found that GABA-immunoreactive ACs were activated at a significantly higher concentration of KA than glycine-immunoreactive ACs (GABA: 38.0 μM, Gly: 30.0 μM). GABA-immunoreactive ACs were also activated at a significantly higher concentration when compared to the total AC population. Half-maximal concentration values for glycine-immunoreactive and total AC population showed overlap in the 95% CI.

The GABA/glycine-immunoreactive AC population constituted only 5.3% of the total of ACs that were responsive to KA (Fig. 10D). The half-maximal KA concentration for this population (23.6 μM) was significantly lower than all other AC populations. Saturating concentrations of KA led to activation of only 60.3% of this population.

Identification of activated ACs with macromolecular markers AC populations that were immunoreactive for bNOS, TH, ChAT, PV, and calretinin were further studied (Fig. 11). bNOS identifies three AC classes in the rat retina, two in the conventional AC layer and one displaced AC (Perez and Caminos, 1995; Chun et al., 1999; Kim et al., 1999, 2000). Saturating concentrations of KA did not activate any of the bNOS-immunoreactive conventional ACs, suggesting that these cells did not express functional KA-responsive glutamate receptors (Fig. 11A–C, white arrowheads). Dopaminergic ACs labeled with TH (Haverkamp and Wässle, 2000) were not activated by a low (5 μM KA) or high (80 μM KA) concentration of KA (Fig. 11D–I, white arrowheads). Cholinergic ACs, immunoreactive for ChAT (Voigt, 1986) showed robust AGB labeling with concentrations of KA as low as 5 μM (Fig. 11J–L, white arrowheads). This was true for both the conventional and displaced AC varieties (52 of 52 cells). AII ACs

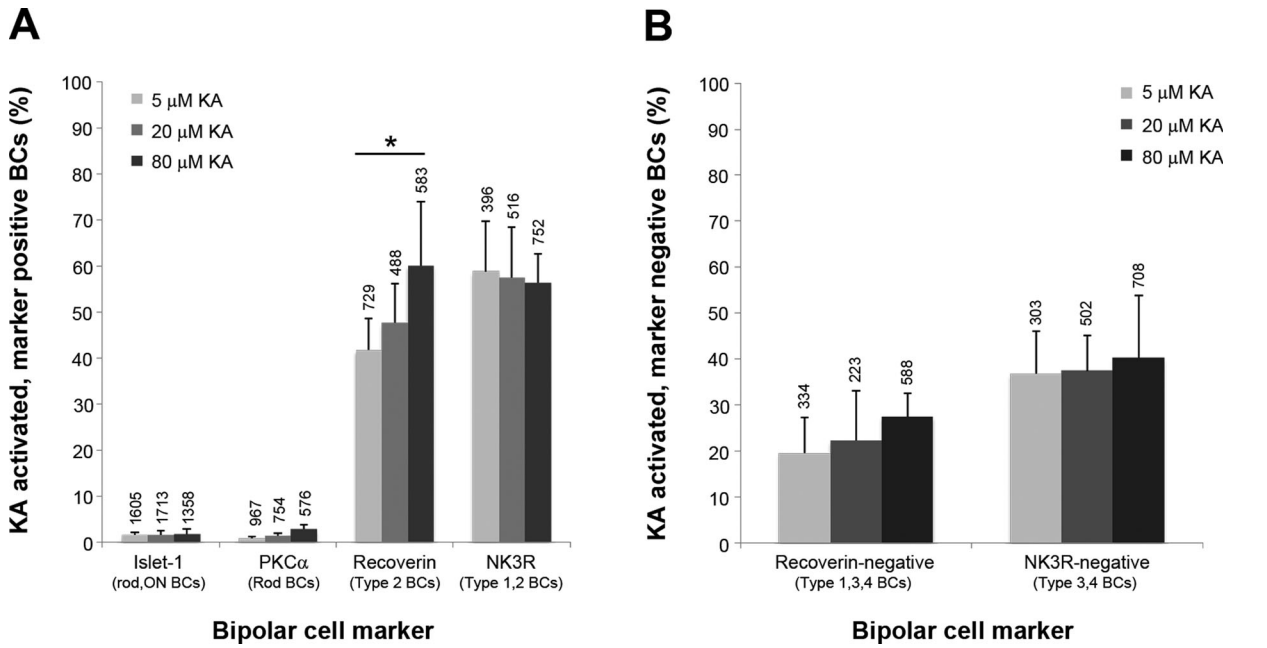

Figure 8. Quantification of kainate (KA)-activated bipolar cell (BC) populations. **A:** Colocalization of KA-activated cells with BC markers. Each column represents the number of activated cells as a percentage of the total number of marker labeled cells. Numbers above each column indicate the total number of cells counted for each marker at that KA concentration, and the asterisk indicates a significant difference (one-way ANOVA, $P < 0.05$). *B:* KA-activated cells void of marker immunoreactivity. Columns represent the number of KA-activated but marker-negative cells as a percentage of all cells activated. Numbers above each column indicate the total number of activated cells (i.e., AGB positive) at that KA concentration. For both figures, data are the mean and SD from five independent rat retinae.

immunolabeled with PV (Wässle et al., 1993) did not show AGB labeling with 5 μM KA (Fig. 11M–O, black arrowheads). Some PV-labeled cells were activated by 20 μM KA (Fig. 11P–R, white arrowheads), and virtually all PV-immunoreactive ACs were activated at 80 μM KA (68 of 68, Fig. 10S–U, white arrowheads). For calretinin-immunoreactive ACs, some were activated at low KA concentrations but not others (Fig. 11V–X, white and black arrowheads, respectively). These activated cells were possibly cholinergic ACs, as they showed similar activation to ChAT-labeled cells. Some calretinin-reactive cells in the ganglion cell layer also colocalized with KA-activated GCs (white arrow), and others did not (black arrow).

Characterization of KA activation within the GC layer

As with ACs, the activation percentage of GCs and displaced ACs displayed a dose-dependent increase with KA. GCs were considered as a separate population from displaced ACs, differentiated according to soma size and amino acid immunoreactivity. The cumulative GC response curve is shown in Figure 12A. At 80 μM KA, 84.6% of all GCs were activated, suggesting that an equal proportion of ACs and GCs express functional glutamate receptors responsive to KA. GCs demonstrated a lower half-maximal concentration compared to ACs of 12.7 μM KA.

KA-activated GCs were largely represented by the Glu/weakly GABA-immunoreactive GCs (52.8%) and Glu-only–immunoreactive GCs (35.1%; Fig. 12B,C). Glu/weakly GABA-immunoreactive GCs were activated at significantly lower KA concentrations compared to Glu-only–immunoreactive GCs. At saturation, 86.7% of Glu/weakly GABA GCs and 73.4% of Glu-only GCs expressed functional KA-sensitive glutamate receptors.

Figure 12D shows that 80.3% of displaced ACs were activated at saturating levels of KA. Displaced AC responses were dominated by the GABA/Glu-immunoreactive ACs. The GABA/Glu-displaced ACs represented 73.7% of all activated displaced ACs. Displaced ACs exhibited a half-maximal KA concentration of 15.5 μM, almost half that of the GABA AC population in the amacrine cell layer (Fig. 10B). This may be due to the high proportion of ChAT ACs present in the displaced AC population, which are highly sensitive to KA (Fig. 11D).

DISCUSSION

KA-responsive glutamate receptors have been observed in BCs, ACs, and GCs in many mammalian retinae (Massey and Miller, 1988; Brandstätter et al., 1994, 1997; Cohen and Miller, 1994; DeVries and Schwartz,

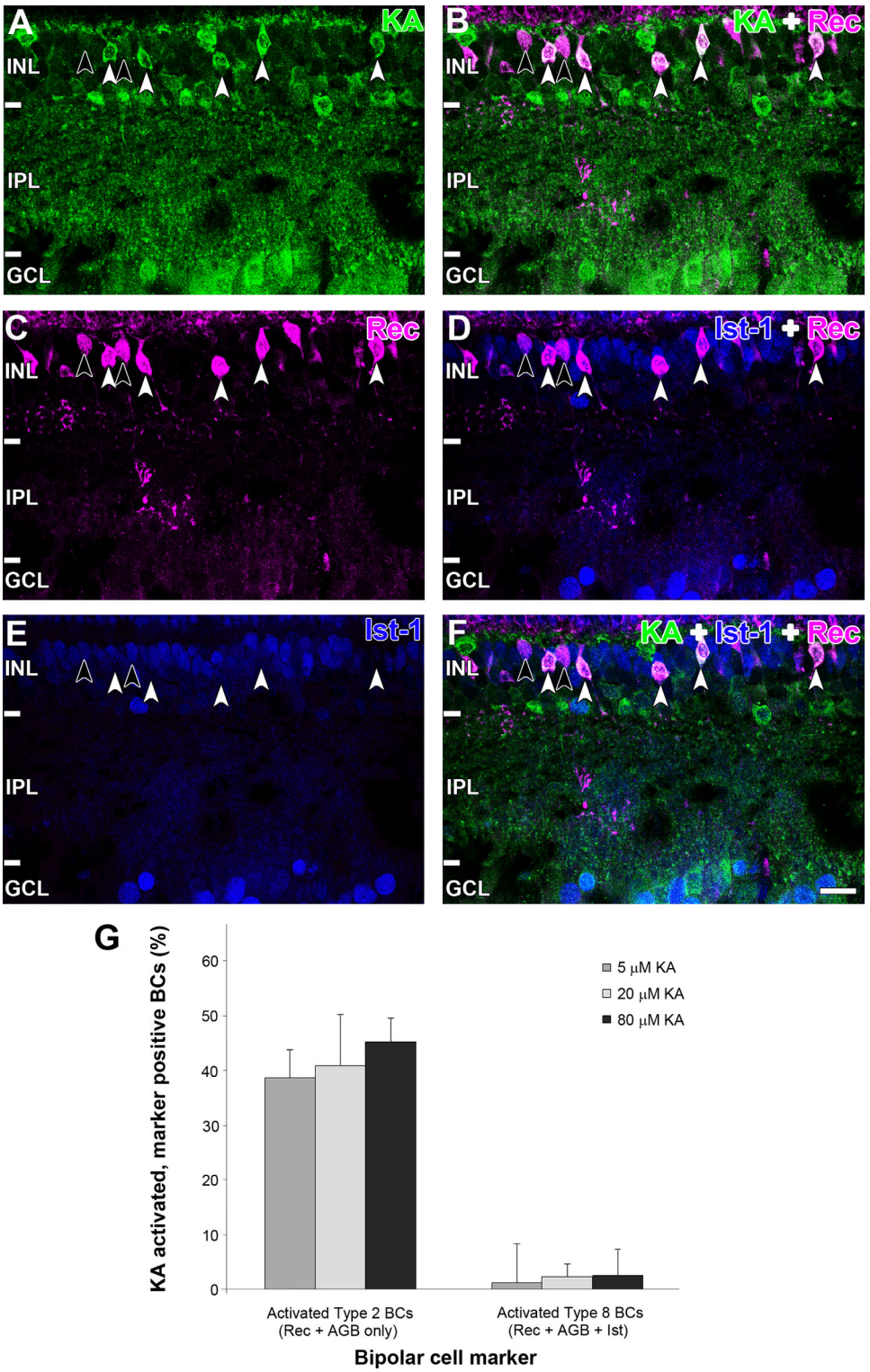

Figure 9. Immunoreactivity of (**A**) AGB (green), (**B**) recoverin (magenta), and (**C**) islet-1 (blue) after activation with 80 μM kainate (KA). **D:** Overlap of AGB and recoverin channels shows that many recoverin BCs were activated by KA (white arrowheads) but not all (black arrowheads). **E:** Overlap of recoverin and Islet-1 channels. Type 8 BCs are identified by colocalization of recoverin and Islet-1 (black arrowheads), and type 2 are identified by the absence of Islet-1 staining (white arrowheads). **F:** Overlap of all three markers. Type 8 BCs are not activated by KA (black arrowheads), whereas type 2 BCs are activated by KA. Retinal layer annotations are the same as in Figure 2. **G:** Quantification of recoverin BC populations with functional KA receptors. The two cell types are presented as a percentage of the total recoverin BC population (5 μM: $n = 735$; 20 μM: $n = 599$; 80 μM: $n = 455$). Each column represents the mean and SD from five independent rat retinae. Abbreviations: Rec, recoverin; Ist-1, islet-1; BC, bipolar cell. Scale bar = 20 μm in F (applies to A–F).

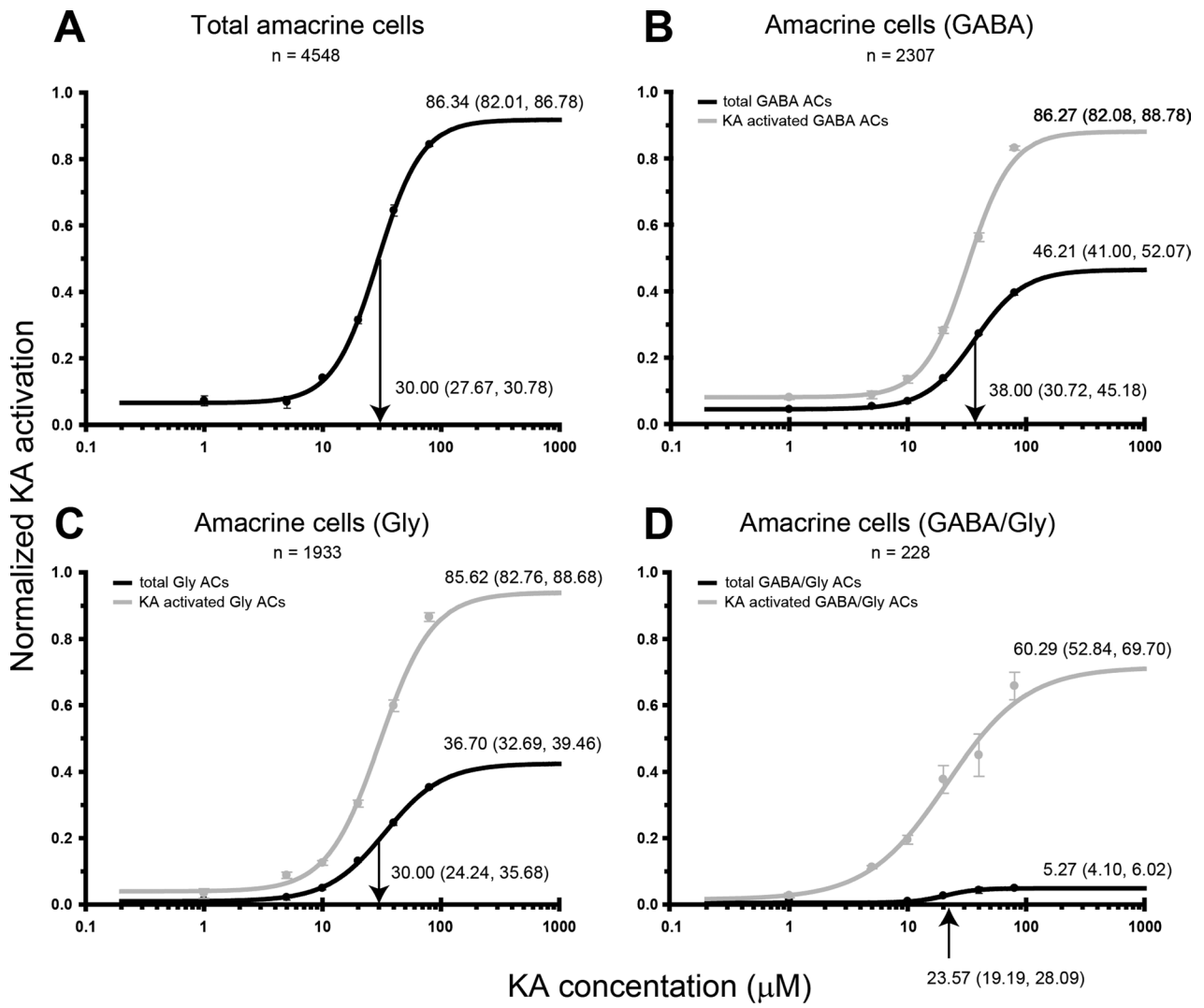

Figure 10. Kainate (KA) dose–response curves for neurochemically distinct AC populations in the inner nuclear layer. Activation curves are presented for (**A**) all amacrine cells (ACs) within the AC layer, (**B**) γ-aminobutyric acid (GABA)-immunoreactive ACs, (**C**) glycine (Gly)-immunoreactive ACs, and (**D**) GABA/Gly-immunoreactive AC populations. The black lines indicate the number KA-activated cells in the cell population as a percentage of the total number of activated cells present. The gray lines indicate the percentage of cells within a neurochemical class that are activated by KA. Activation curve annotations and axes labeling are as described in Figure 3.

TABLE 2.

Summary of KA Activation Curve Characteristics for Cell Populations of the Rat Inner Retina[1]

Cell class	R_{max}	n	K
Amacrine cells			
Total	86.34 (82.01, 86.78)	0.034 (0.031, 0.038)	30.00 (27.67, 30.78)
GABA	46.21 (41.00, 52.07)	0.023 (0.019, 0.032)	38.00 (30.72, 45.18)
Glycine	36.70 (32.69, 39.46)	0.036 (0.028, 0.044)	30.00 (24.24, 35.68)
GABA/Glycine	5.27 (4.10, 6.02)	0.050 (0.027, 0.065)	23.57 (19.19, 28.09)
Ganglion cells			
Total	84.56 (83.31, 85.75)	0.071 (0.064, 0.080)	12.70 (11.83, 13.33)
Glu	35.13 (30.26, 35.98)	0.038 (0.031, 0.072)	23.00 (13.92, 26.65)
Glu/weakly GABA	52.75 (51.08, 54.54)	0.078 (0.066, 0.089)	11.42 (10.16, 12.71)
Displaced amacrine cells			
Glu/GABA	73.70 (71.92, 75.39)	0.061 (0.053, 0.069)	15.50 (14.05, 17.23)

[1] R_{max} represents the total percentage of cells in the class activated at saturating KA levels (80 μM), n represents the slope parameter, and K represents the concentration of KA that activates half of the cell class. Values are presented as mean and bounds of four rat retinae using a 95% confidence interval.

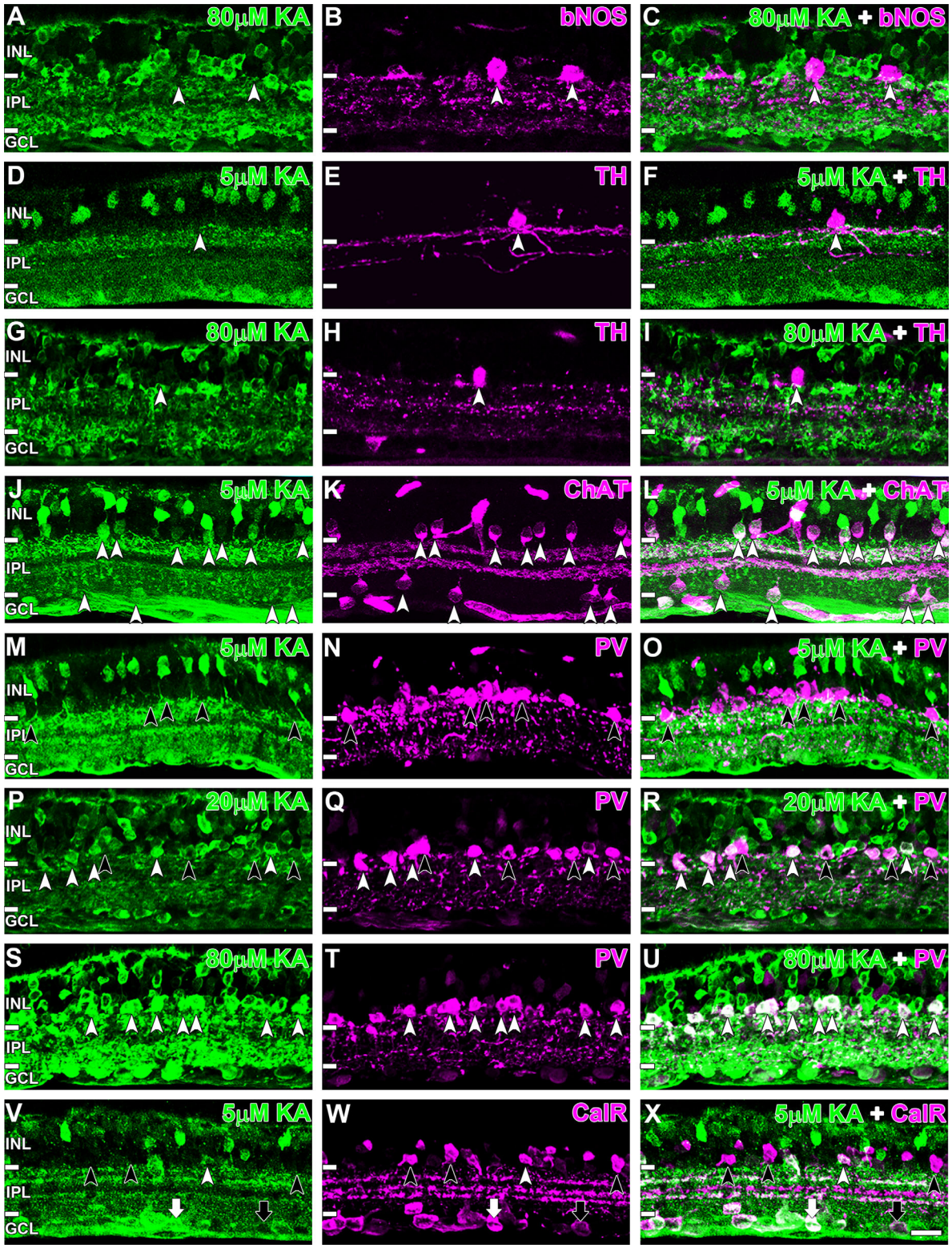

Figure 11. Kainate (KA) activation of immunocytochemically identified AC populations. **A–C:** Brain nitric oxide synthase (bNOS)-immunoreactive ACs were not activated by KA even at saturating levels (white arrowheads). **D–F:** Tyrosine hydroxylase (TH)-immunoreactive ACs also did not colocalize with KA-activated ACs at low or saturating KA concentrations (white arrowheads). **G–I:** Colocalization was evident between AGB and choline acetyltranferase (ChAT)-reactive ACs (white arrowheads). M–U: Parvalbumin (PV)-positive ACs were activated with KA concentrations exceeding 5 μM. **M–O:** No colocalization was observed for incubations with 5 μM KA (black arrowheads). **P–R:** At 20 μM, most PV ACs were colocalized (white arrowheads), but some remained AGB negative (black arrowheads). **S–U:** All PV-immunoreactive cells were colocalized with KA-activated cells at 80 μM (white arrowheads). **V–X:** Colocalization with KA-activated cells was observed for some calretinin-positive ACs (white arrowheads) but not others (black arrowheads). Similarly, some calretinin-reactive cells in the ganglion cell layer colocalized with KA-activated GCs (white arrow) and others did not (black arrow). Retinal layer annotations are the same as in Figure 2. Scale bar = 20 μm in X (applies to A–X).

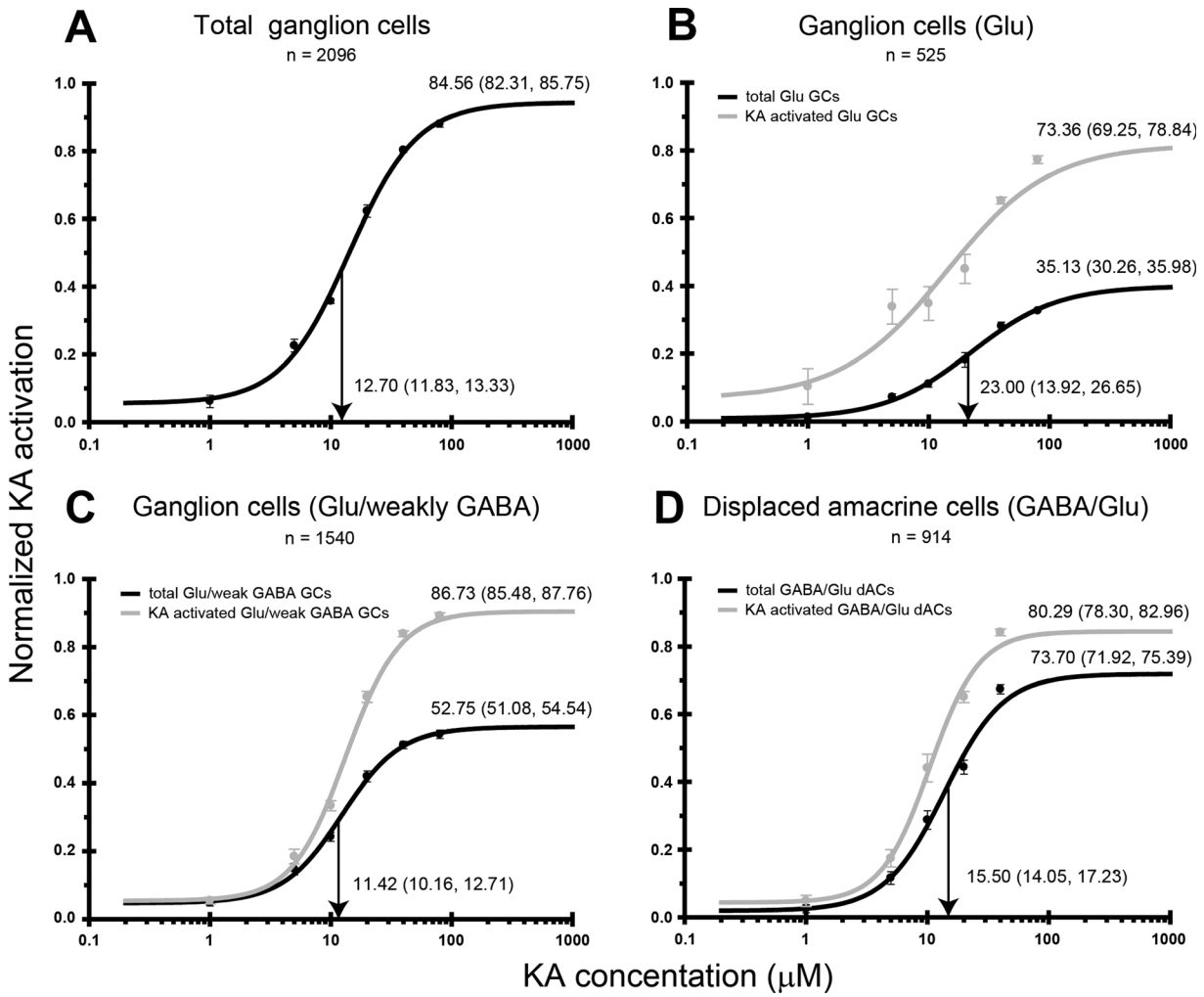

Figure 12. Kainate (KA) dose–response curves for neurochemically distinct cell populations in the ganglion cell layer. Activation curves are presented for (**A**) all ganglion cells (GCs) within the ganglion cell layer, (**B**) glutamate (Glu)-immunoreactive GCs, (**C**) Glu/weakly γ-aminobutyric acid (GABA)-immunoreactive GCs, and (**D**) displaced amacrine cells (ACs). The black lines indicate the number of KA-activated cells in the cell population as a percentage of the total number of activated cells present. The gray lines indicate the percentage of cells within a neurochemical class that are activated by KA. Activation curve annotations and axes labeling are as described in Figure 3.

1999; Marc, 1999a; Haverkamp et al., 2001; Qin and Pourcho, 2001). This study has quantified the proportion of neurochemically classified cells expressing functional KA-sensitive glutamate receptors based on the entry of the organic cation AGB. We first determined overall cell activation patterns by using amino acid labeling and cell morphometrics followed by the use of macromolecular markers to focus on subpopulations of neurons.

Figure 13 summarizes the differences in KA sensitivity of the neuronal populations investigated in this study. The clear distinction in KA activation levels of BCs, ACs, and GCs suggests that although many inner retinal neurons express glutamate receptors responsive to KA, receptor kinetics are not equivalent between cell classes. In vitro expression studies indicate that KA affinity of glutamate receptors is dictated by receptor subunit composition (Herb et al., 1992). This would explain differences in subunit expression in the rat retina, with some KA subunits localized throughout the inner nuclear and ganglion cell layers (i.e., KA2, GluR7) and others restricted to certain strata (i.e., GluR5 to the outer half of the inner nuclear layer; Brandstätter et al., 1994, 1997). A similar model has been proposed for differences observed in NMDA thresholds of ACs and GCs in the rat retina (Sun et al., 2003).

AGB as a probe of glutamate receptor function

The use of AGB as a probe of ion flow was instigated by Yoshikami (1981) using autoradiography and subsequently applied to the retina through immunodetection by Marc (1999a,b). The theoretical framework has been

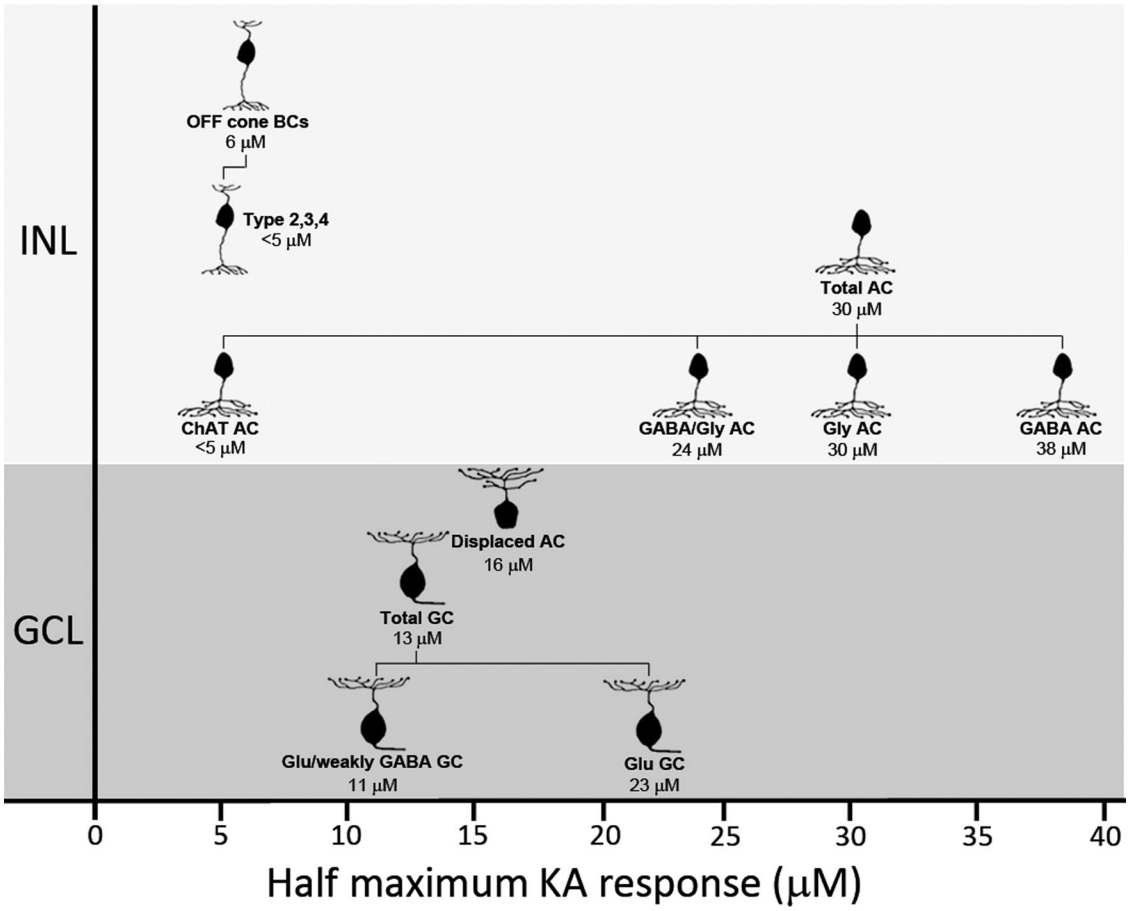

Figure 13. Diagrammatic representation of kainate (KA) sensitivity of various neurochemically identified cell populations in the rat inner retina. Annotations below cell images indicate the neurochemical cell class and the half-maximal activation concentration for that class. Data are based on dose activation curves in Figures 3, 10, and 12. For Chat ACs and type 2, 3, and 4 BCs, estimates of half-maximum concentration have been made from immunolabeling. Abbreviations: INL, inner nuclear layer; GCL, ganglion cell layer; BC, bipolar cell; AC, amacrine cell; GC, ganglion cell; GABA, γ-aminobutyric acid; Gly, glycine; Glu, glutamate.

reviewed in the past (Marc, 1999b,c; Marc et al., 2005; Sun and Kalloniatis, 2006). AGB labeling secondary to endogenous (basal) or exogenous (ligand) activation reports on the cation entry history of the cell and not the summed excitation/inhibitory history (Marc et al., 2005). Guanidinium compounds like AGB permeate cation channels and are immunodetectable when only a small fraction of glutamate receptors have been activated (Picco and Menini, 1993; Marc et al., 2005) using short incubation times secondary to ligand activation (Marc, 1999a,b; Michel et al., 1999; Edwards and Michel, 2003; Marc et al., 2005; Sun and Kalloniatis, 2006; Acosta et al., 2007; Edwards et al., 2007; Chang and Chiao, 2008; Mobley et al., 2008; Chang et al., 2010; Chen and Chiao, 2012). Factors that will affect AGB labeling include cell volume, channel size, number of open channels, ligand affinity of receptor channel, channel permeation, and channel desensitization (Marc, 1999a,b; Marc et al., 2005; Sun and Kalloniatis, 2006).

The use of AGB labeling as a probe of functional glutamate receptors requires careful interpretation. KA is known to activate AMPA receptors at high concentrations (Sommer and Seeburg, 1992; Paternain et al., 1995), and thus recruitment of non-KA receptors is possible. Soma labeling is also possible secondary to mechanical disruption (Marc, 1999a,b); however, this and previous studies indicated that such labeling will be below ~5–8%—the error in labeling ON bipolar cells secondary to ionotropic receptor activation (Sun and Kalloniatis, 2006).

Response of BCs to KA

Approximately 30% of rat BCs were activated by KA, and this population was comprised almost exclusively of OFF cone BCs. This agrees with previous studies that estimate 25% of BCs in the rat retina as OFF cone BCs (Euler and Wässle, 1995; Kamphuis et al., 2003; Sun et al., 2007a). The absence of AGB in immunolabeled rod and

ON cone BCs further confirmed that KA activation was limited to OFF cone BCs. Four OFF cone BC subtypes, types 1, 2, 3, and 4, with relatively even distributions, have been proposed in the rat (Euler and Wässle, 1995; Hartveit, 1997; Masland, 2001a,b). The KA responsiveness of each cell type, however, is unknown. In the rabbit retina, OFF cone BCs show heterogeneous responses to KA, suggesting different KA-sensitive glutamate receptors between OFF cone BC subtypes (Marc, 1999a). The high level of OFF cone BC activation (88.4%) observed in this study points to the likelihood of all four rat OFF cone BC types being activated by high levels of KA. This does not imply that all OFF cone BCs display KA receptors, but rather that all are activated with KA. KA is known to activate AMPA receptors at higher concentrations (Sommer and Seeburg, 1992; Paternain et al., 1995), and thus, OFF cone BCs activated at low KA concentrations likely reflect the populations that have KA-only receptors.

Recoverin labeling indicated that type 2 BCs present functional KA-responsive glutamate receptors in the rat. Although only ~56% of the recoverin BCs were activated at saturating KA levels, overlap with ON cone BC markers confirmed that the majority of inactivated recoverin cells were type 8 ON BCs. Previous studies have estimated that 65% and 35% of recoverin BCs are types 2 and 8, respectively (Euler and Wässle, 1995; Kamphuis et al., 2003). Thus, activation of 56% of recoverin cells suggests that almost all type 2 BCs are KA responsive. The significant increase in activated cells with KA concentration suggests variability in KA sensitivity within this population. DeVries (2000) showed that two OFF BC types in the ground squirrel (b3 and b7), which were both sensitive to KA, varied in desensitization response and recovery times. Even so, 42 ± 7.0% of recoverin BCs were activated at 5 μM KA, indicating that a large proportion of type 2 BCs are highly KA sensitive.

For NK3R-reactive BCs (types 1 and 2), ~56% of this population was activated at saturating KA concentrations. This was not significantly different from the recoverin BCs population ($P = 0.96$). As recoverin immunoreactivity suggests that most type 2 BCs are KA sensitive, it is possible that the inactivated NK3R population consists of type 1 BCs. Similarly to recoverin OFF cone BCs, NK3R cells were highly sensitive to low KA concentrations, further suggesting this population to be type 2 BCs. Unfortunately, overlap of antibody hosts meant we were unable to combine NK3R and recoverin markers to differentiate between types 1 and 2 BCs in this study. Studies in the mouse, however, indicate that types 1 and 2 BCs do differ in activation characteristics. Type 1 mouse BCs appear to avoid S-cones and may be exclusively involved in the green OFF pathway, whereas type 2 BCs form nonselective cone contacts (Breuninger et al., 2011; Puller and Haverkamp, 2011). Type 1 mouse BCs and recoverin-negative (i.e., types 1, 3, or 4 but not type 2) BCs in the rat retina also exclusively express the AMPA receptor subunit GluR1 (Kamphuis et al., 2003; Breuninger et al., 2011).

Electrophysiological studies suggest that neurons unresponsive to KA may use AMPA receptors. DeVries (2000) showed that OFF BCs in the ground squirrel retina, which were not activated by KA, were highly responsive to AMPA, suggesting that OFF BCs may use only one receptor type as a way to filter visual signals (DeVries, 2000). In this study, we could not assign AMPA receptors to BC populations that were unresponsive to KA, as only a single glutamate receptor agonist was used. KA also induces nondesensitizing responses from AMPA receptors, and thus at saturating concentrations, AGB-labeled cells may arise from nonspecific activation of AMPA receptors (Sommer and Seeburg, 1992; Paternain et al., 1995). We are currently performing studies with AMPA, GYKI53655 (a selective AMPA receptor antagonist), and SYM2081 (a selective KA receptor agonist) to resolve the ambiguity of glutamate receptor functionality.

KA can also desensitize KA receptors (Jones et al., 1997); however, this is less likely to affect this study as the AGB technique measures the accumulation of the cation in activated cells and only a fraction of channels need to be open for detectable levels of AGB (Marc et al., 2005). We also used a binary classification system when counting cells that did not rely on quantitative difference in AGB entry, but rather on whether glutamate channels were functional or not (Sun and Kalloniatis, 2006; Acosta et al., 2007).

Analysis of types 3 and 4 BCs was limited in this study by the availability of reliable immunocytochemical rat BC markers. Markers for these cells have been identified in the mouse (Haeseleer et al., 2000; Haverkamp et al., 2003, 2008; Ghosh et al., 2004; Mataruga et al., 2007; Puthussery et al., 2010), but their reactivity in the rat is either absent or yet to be shown. Other markers, such as hyper polarization-activated cyclic nucleotide-gated channel 4 (HCN4), which identifies type 3 rat OFF cone BCs (Fyk-Kolodziej and Pourcho, 2007), display immunoreactivity mostly localized to cell axons and dendrites, making it difficult to reliably match with the predominantly soma-based AGB labeling. We assessed types 3 and 4 BCs through the absence of NK3R or recoverin labeling. At saturating KA concentrations, 40 ± 5.0% of activated OFF cone BCs were NK3R immunonegative, indicating that at least one of these cell types is responsive to KA. Activation of recoverin-negative OFF BCs (types 1, 3, and 4) was not significantly different from the NK3R-immunonegative population, further suggesting that type 1 OFF BCs are not responsive to KA.

Response of ACs and GCs to KA

Cells of the inner nuclear and ganglion cell layer responded to KA dose dependently. Virtually all ACs (86%) showed AGB entry, implying functional KA-sensitive glutamate receptors on most rat ACs. The half-maximal KA concentration for ACs was 30 μM KA, matching values observed for ACs in the rabbit (Marc, 1999b).

The majority of KA-responsive ACs could be divided equally between the GABA- and glycine-immunoreactive populations. The wide range of responses in the GABAergic population is likely to reflect the heterogeneity within this group (Pourcho and Goebel, 1983; Marc, 1999a). Cholinergic ACs were the most KA-sensitive GABAergic cell population matching data from the rabbit retina, in which cholinergic ACs were strongly activated with only 6 μM KA (Marc, 1999a,b). Toxicity studies also indicate high KA sensitivity in cholinergic ACs (Osborne et al., 1995).

TH- and bNOS-immunoreactive ACs contributed to the ~14% GABAergic ACs that were unresponsive to KA. TH-immunoreactive ACs that are dopaminergic (Oyster et al., 1985) are also resistant to KA toxicity in the rabbit and the chicken retina (Ingham and Morgan, 1983; Morgan, 1983; Marc, 1999a). Excitotoxicity studies in the rat retina, however, demonstrate conflicting results including KA-induced cell death of TH cells (Park et al., 2005; Cheon et al., 2006). Similarly, bNOS-immunoreactive ACs were unresponsive to KA in our study but showed sensitivity to KA toxicity in the rabbit retina (Sagar, 1990). In the toxicity studies, cell death occurred 7–10 days after KA administration, and therefore this effect may not be directly due to KA-sensitive receptors on TH- and bNOS-immunoreactive cells. bNOS-immunoreactive cells also show KA-induced GABA release in the primate retina (Andrade da Costa et al., 2001), but this discrepancy may be related to species-specific differences between primate and rat bNOS-reactive cells. Species differences may also explain loss of light responses in mouse TH-immunoreactive cells after administration of a KA antagonist (Pang et al., 2010). Additionally, Pang et al. (2010) abolished light responses by using DNQX, an antagonist to non-NMDA receptors (Honore et al., 1988), and therefore these effects cannot be specifically attributed to KA-sensitive receptors on TH-immunoreactive cells. The theoretical calculations by Marc et al. (2005) suggest that our experimental paradigm should have resulted in detectable AGB levels if these cells had KA/AMPA receptors on their membranes.

For the glycinergic AC population, the characteristics of the dose–response curve (~43% activation at 30 μM KA; ~86% activation at 80 μM KA) closely matched the immunolabeling of AII ACs by PV (partial colocalization at 20 μM KA; complete colocalization at 80 μM KA). This suggests that the AII AC population makes a considerable contribution to the glycinergic AC response. Indeed, AII ACs are the predominant glycinergic AC type (MacNeil and Masland, 1998; MacNeil et al., 2009). In the rabbit retina, AII ACs also contributed most to the glycinergic AC response (Marc, 1999a). Dumitrescu et al. (2006) showed that 77% of mice AII ACs possessed AMPA- and KA-responsive glutamate receptors but AII ACs did not express KA-responsive glutamate receptors exclusively. Electrophysical recordings from the rat and rabbit retina also indicate that AII ACs only possess functional AMPA receptors (Morkve et al., 2002; Veruki et al., 2003; Zhou and Dacheux, 2004). Immunocytochemical staining of AII ACs in the macaque monkey and rabbit retina found AMPA receptor subunits GluR 2/3 and 4 postsynaptic to rod BCs (Ghosh et al., 2001). Thus, activation of these cells by KA in this study may be due to nonspecific activation of AMPA receptors on these cells rather than glutamate receptors responsive to KA (Sommer and Seeburg, 1992; Paternain et al., 1995). Further work is needed to determine ionotropic glutamate receptor functionality for these cells.

In the ganglion cell layer, most GCs (~85%) were KA responsive, similar to the rabbit (Massey and Miller, 1988; Marc, 1999a), cat (Cohen et al., 1994), and primate (Cohen and Miller, 1994; Zhou et al., 1994). Sun et al. (2003) found that 87% of GCs were activated with NMDA, suggesting equal use of non-NMDA and NMDA receptors by these cells (Sun et al., 2003). Lack of available selective GC markers limited segregation to amino acid profiles. Glu GCs were more sensitive to Glu/weakly GABA than to KA, similar to previous work in the rabbit (Marc, 1999a).

CONCLUSIONS

Numerous reports suggest that differences in neurotransmitter receptor sensitivity constitute a mechanism for filtering and delineating signal pathways (DeVries, 2000; Li and DeVries, 2006; Breuninger et al., 2011). This study sought to further understand these pathways by ascribing functional KA-sensitive glutamate receptors to specific cell subpopulations of the inner retina. Beyond understanding signaling pathways, knowledge of receptor sensitivity also provides a roadmap to cell susceptibility to glutamate neurotoxicity. The pathology of retinal conditions such as ischemia is associated with excessive stimulation of glutamate receptors (Lipton and Rosenberg, 1994; Robin and Kalloniatis, 1992). Whereas NMDA receptors are predominantly implicated in glutamate toxicity, KA-sensitive receptors may also promote cell death (Sucher et al., 1997). OFF BCs are highly sensitive to KA and

therefore are probably at the greatest risk of KA toxicity, followed by GCs (Fig. 13). Thus monitoring for dysfunction in these cells may show an early indication of glutamate toxicity.

CONFLICT OF INTEREST STATEMENT

All the authors certify that there is no conflict of interest regarding the material presented in this manuscript. R.E. Marc is Chief Executive Officer of Signature Immunologics.

ROLE OF AUTHORS

All authors had full access to all the data in the study and take responsibility for the integrity of the data and the accuracy of the data analysis. Study concept and design: L. Nivison-Smith, D. Sun, E.L. Fletcher, and M. Kalloniatis. Acquisition of data: L. Nivison-Smith, D. Sun, and R.E. Marc. Analysis and interpretation of data: L. Nivison-Smith, D. Sun, and M. Kalloniatis. Drafting of the manuscript: L. Nivison-Smith and D. Sun. Critical revision of the manuscript for important intellectual content: E.L. Fletcher, R.E. Marc, and M. Kalloniatis. Statistical analysis: L. Nivison-Smith and D. Sun. Obtained funding: E.L. Fletcher, M. Kalloniatis, and R.E. Marc. Administrative, technical, and material support: R.E. Marc. Study supervision: M. Kalloniatis

LITERATURE CITED

Acosta ML, Chua J, Kalloniatis M. 2007. Functional activation of glutamate ionotropic receptors in the developing mouse retina. J Comp Neurol 500:923–941.

Andrade da Costa BL, de Mello FG, Hokoc JN. 2001. Comparative study of glutamate mediated gamma-aminobutyric acid release from nitric oxide synthase and tyrosine hydroxylase immunoreactive cells of the *Cebus apella* retina. Neurosci Lett 302:21–24.

Brandstätter JH, Hartveit E, Sassoe-Pognetto M, Wässle H. 1994. Expression of NMDA and high-affinity kainate receptor subunit mRNAs in the adult rat retina. Eur J Neurosci 6:1100–1112.

Brandstätter JH, Koulen P, Wässle H. 1997. Selective synaptic distribution of kainate receptor subunits in the two plexiform layers of the rat retina. J Neurosci 17:9298–9307.

Breuninger T, Puller C, Haverkamp S, Euler T. 2011. Chromatic bipolar cell pathways in the mouse retina. J Neurosci 31:6504–6517.

Bui BV, Weisinger HS, Sinclair AJ, Vingrys AJ. 1998. Comparison of guinea pig electroretinograms measured with bipolar corneal and unipolar intravitreal electrodes. Doc Ophthalmol 95:15–34.

Bui BV, Edmunds B, Cioffi GA, Fortune B. 2005. The gradient of retinal functional changes during acute intraocular pressure elevation. Invest Ophthalmol Vis Sci 46:202–213.

Casini G, Brecha NC, Bosco L, Rickman DW. 2000. Developmental expression of neurokinin-1 and neurokinin-3 receptors in the rat retina. J Comp Neurol 421:275–287.

Chang YC, Chiao CC. 2008. Localization and functional mapping of AMPA receptor subunits in the developing rabbit retina. Invest Ophthalmol Vis Sci 49:5619–5628.

Chang YC, Chen CY, Chiao CC. 2010. Visual experience-independent functional expression of NMDA receptors in the developing rabbit retina. Invest Ophthalmol Vis Sci 51: 2744–2754.

Chen YP, Chiao CC. 2012. Functional expression of ionotropic glutamate receptors in the rabbit retinal ganglion cells. Brain Res 1427:10–22.

Cheon EW, Park CH, Kim YS, Cho CH, Chung YC, Kwon JG, Yoo JM, Choi WS, Cho GJ. 2006. Protective effects of betaxolol in eyes with kainic acid-induced neuronal death. Brain Res 1069:75–85.

Chun MH, Oh SJ, Kim IB, Kim KY. 1999. Light and electron microscopical analysis of nitric oxide synthase-like immunoreactive neurons in the rat retina. Vis Neurosci 16: 379–389.

Cohen ED, Miller RF. 1994. The role of NMDA and non-NMDA excitatory amino acid receptors in the functional organization of primate retinal ganglion cells. Vis Neurosci 11: 317–332.

Cohen ED, Zhou ZJ, Fain GL. 1994. Ligand-gated currents of alpha and beta ganglion cells in the cat retinal slice. J Neurophysiol 72:1260–1269.

Crooks J, Kolb H. 1992. Localization of GABA, glycine, glutamate and tyrosine hydroxylase in the human retina. J Comp Neurol 315:287–302.

Darvas F, Pantazis D, Kucukaltun-Yildirim E, Leahy RM. 2004. Mapping human brain function with MEG and EEG: methods and validation. Neuroimage 23(suppl 1):S289–S299.

Davanger S, Ottersen OP, Storm-Mathisen J. 1991. Glutamate, GABA, and glycine in the human retina: an immunocytochemical investigation. J Comp Neurol 311:483–494.

DeVries SH. 2000. Bipolar cells use kainate and AMPA receptors to filter visual information into separate channels. Neuron 28:847–856.

DeVries SH, Schwartz EA. 1999. Kainate receptors mediate synaptic transmission between cones and 'Off' bipolar cells in a mammalian retina. Nature 397:157–160.

Dinerman JL, Dawson TM, Schell MJ, Snowman A, Snyder SH. 1994. Endothelial nitric oxide synthase localized to hippocampal pyramidal cells: implications for synaptic plasticity. Proc Natl Acad Sci U S A 91:4214–4218.

Dingledine R, Borges K, Bowie D, Traynelis SF. 1999. The glutamate receptor ion channels. Pharmacol Rev 51:7–61.

Dumitrescu ON, Protti DA, Majumdar S, Zeilhofer HU, Wässle HU. 2006. Ionotropic glutamate receptors of amacrine cells of the mouse retina. Vis Neurosci 23:79–90.

Edwards FA, Konnerth A, Sakmann B, Takahashi T. 1989. A thin slice preparation for patch clamp recordings from neurones of the mammalian central nervous system. Pflugers Arch 414:600–612.

Edwards JG, Michel WC. 2003. Pharmacological characterization of ionotropic glutamate receptors in the zebrafish olfactory bulb. Neuroscience 122:1037–1047.

Edwards JG, Greig A, Sakata Y, Elkin D, Michel WC. 2007. Cholinergic innervation of the zebrafish olfactory bulb. J Comp Neurol 504:631–645.

Efron B, Tibshirani R. 1986. Bootstrap methods for standard errors, confidence intervals, and other measures of statistical accuracy. Stat Sci 1:54–75.

Euler T, Wässle H. 1995. Immunocytochemical identification of cone bipolar cells in the rat retina. J Comp Neurol 361: 461–478.

Foster DH, Bischof WF. 1987. Bootstrap variance estimators for the parameters of small-sample sensory-performance functions. Biol Cybern 57:341–347.

Fyk-Kolodziej B, Pourcho RG. 2007. Differential distribution of hyperpolarization-activated and cyclic nucleotide-gated

channels in cone bipolar cells of the rat retina. J Comp Neurol 501:891–903.
Ghosh KK, Haverkamp S, Wässle H. 2001. Glutamate receptors in the rod pathway of the mammalian retina. J Neurosci 21:8636–8647.
Ghosh KK, Bujan S, Haverkamp S, Feigenspan A, Wässle H. 2004. Types of bipolar cells in the mouse retina. J Comp Neurol 469:70–82.
Grady EF, Baluk P, Bohm S, Gamp PD, Wong H, Payan DG, Ansel J, Portbury AL, Furness JB, McDonald DM, Bunnett NW. 1996. Characterization of antisera specific to NK1, NK2, and NK3 neurokinin receptors and their utilization to localize receptors in the rat gastrointestinal tract. J Neurosci 16:6975–6986.
Greferath U, Grünert U, Wässle H. 1990. Rod bipolar cells in the mammalian retina show protein kinase C-like immunoreactivity. J Comp Neurol 301:433–442.
Hack I, Peichl L, Brandstätter JH. 1999. An alternative pathway for rod signals in the rodent retina: rod photoreceptors, cone bipolar cells, and the localization of glutamate receptors. Proc Natl Acad Sci U S A 96:14130–14135.
Haeseleer F, Sokal I, Verlinde CL, Erdjument-Bromage H, Tempst P, Pronin AN, Benovic JL, Fariss RN, Palczewski K. 2000. Five members of a novel Ca(2+)-binding protein (CABP) subfamily with similarity to calmodulin. J Biol Chem 275:1247–1260.
Hamassaki-Britto DE, Hermans-Borgmeyer I, Heinemann S, Hughes TE. 1993. Expression of glutamate receptor genes in the mammalian retina: the localization of GluR1 through GluR7 mRNAs. J Neurosci 13:1888–1898.
Hartveit E. 1997. Functional organization of cone bipolar cells in the rat retina. J Neurophysiol 77:1716–1730.
Haverkamp S, Wässle H. 2000. Immunocytochemical analysis of the mouse retina. J Comp Neurol 424:1–23.
Haverkamp S, Grünert U, Wässle H. 2001. Localization of kainate receptors at the cone pedicles of the primate retina. J Comp Neurol 436:471–486.
Haverkamp S, Ghosh KK, Hirano AA, Wässle H. 2003. Immunocytochemical description of five bipolar cell types of the mouse retina. J Comp Neurol 455:463–476.
Haverkamp S, Specht D, Majumdar S, Zaidi NF, Brandstätter JH, Wasco W, Wässle H, Tom Dieck S. 2008. Type 4 OFF cone bipolar cells of the mouse retina express calsenilin and contact cones as well as rods. J Comp Neurol 507: 1087–1101.
Haycock JW. 1987. Stimulation-dependent phosphorylation of tyrosine hydroxylase in rat corpus striatum. Brain Res Bull 19:619–622.
Heizmann CW, Celio MR. 1987. Immunolocalization of parvalbumin. Methods Enzymol 139:552–570.
Herb A, Burnashev N, Werner P, Sakmann B, Wisden W, Seeburg PH. 1992. The KA-2 subunit of excitatory amino acid receptors shows widespread expression in brain and forms ion channels with distantly related subunits. Neuron 8:775–785.
Hollmann M, Heinemann S. 1994. Cloned glutamate receptors. Annu Rev Neurosci 17:31–108.
Honore T, Davies SN, Drejer J, Fletcher EJ, Jacobsen P, Lodge D, Nielsen FE. 1988. Quinoxalinediones: potent competitive non-NMDA glutamate receptor antagonists. Science 241:701–703.
Hughes TE, Hermans-Borgmeyer I, Heinemann S. 1992. Differential expression of glutamate receptor genes (GluR1–5) in the rat retina. Vis Neurosci 8:49–55.
Ingham CA, Morgan IG. 1983. Dose-dependent effects of intravitreal kainic acid on specific cell types in chicken retina. Neuroscience 9:165–181.
Jones BW, Kondo M, Terasaki H, Watt CB, Rapp K, Anderson J, Lin Y, Shaw MV, Yang JH, Marc RE. 2011. Retinal remodeling in the Tg P347L rabbit, a large-eye model of retinal degeneration. J Comp Neurol 519:2713–2733.
Jones KA, Wilding TJ, Huettner JE, Costa AM. 1997. Desensitization of kainate receptors by kainate, glutamate and diastereomers of 4-methylglutamate. Neuropharmacology 36: 853–863.
Kalloniatis M, Fletcher EL. 1993. Immunocytochemical localization of the amino acid neurotransmitters in the chicken retina. J Comp Neurol 336:174–193.
Kalloniatis M, Marc RE, Murry RF. 1996. Amino acid signatures in the primate retina. J Neurosci 16:6807–6829.
Kalloniatis M, Tomisich G, Wellard JW, Foster LE. 2002. Mapping photoreceptor and postreceptoral labelling patterns using a channel permeable probe (agmatine) during development in the normal and RCS rat retina. Vis Neurosci 19:61–70.
Kalloniatis M, Sun D, Foster L, Haverkamp S, Wässle H. 2004. Localization of NMDA receptor subunits and mapping NMDA drive within the mammalian retina. Vis Neurosci 21:587–597.
Kamphuis W, Klooster J, Dijk F. 2003. Expression of AMPA-type glutamate receptor subunit (GluR2) in ON-bipolar neurons in the rat retina. J Comp Neurol 455:172–186.
Kim IB, Lee EJ, Kim KY, Ju WK, Oh SJ, Joo CK, Chun MH. 1999. Immunocytochemical localization of nitric oxide synthase in the mammalian retina. Neurosci Lett 267: 193–196.
Kim KY, Ju WK, Oh SJ, Chun MH. 2000. The immunocytochemical localization of neuronal nitric oxide synthase in the developing rat retina. Experimental brain research Experimentelle Hirnforschung Experimentation cerebrale 133:419–424.
Li W, DeVries SH. 2006. Bipolar cell pathways for color and luminance vision in a dichromatic mammalian retina. Nat Neurosci 9:669–675.
Lipton SA, Rosenberg PA. 1994. Excitatory amino acids as a final common pathway for neurologic disorders. N Engl J Med 330:613–622.
MacNeil MA, Masland RH. 1998. Extreme diversity among amacrine cells: implications for function. Neuron 20: 971–982.
MacNeil MA, Purrier S, Rushmore RJ. 2009. The composition of the inner nuclear layer of the cat retina. Vis Neurosci 26:365–374.
Marc RE. 1999a. Kainate activation of horizontal, bipolar, amacrine, and ganglion cells in the rabbit retina. J Comp Neurol 407:65–76.
Marc RE. 1999b. Mapping glutamatergic drive in the vertebrate retina with a channel-permeant organic cation. J Comp Neurol 407:47–64.
Marc RE. 1999c.Subtypes of off-center bipolar cells possess different ionotropic glutamate receptor channel properties. Invest Ophthalmol Vis Sci 40:S790.
Marc RE, Jones BW. 2002. Molecular phenotyping of retinal ganglion cells. J Neurosci 22:413–427.
Marc RE, Liu WL, Kalloniatis M, Raiguel SF, van Haesendonck E. 1990. Patterns of glutamate immunoreactivity in the goldfish retina. J Neurosci 10:4006–4034.
Marc RE, Murry RF, Basinger SF. 1995. Pattern recognition of amino acid signatures in retinal neurons. J Neurosci 15: 5106–5129.
Marc RE, Kalloniatis M, Jones BW. 2005. Excitation mapping with the organic cation AGB2+. Vision Res 45:3454–3468.
Masland RH. 2001a. The fundamental plan of the retina. Nat Neurosci 4:877–886.
Masland RH. 2001b. Neuronal diversity in the retina. Curr Opin Neurobiol 11:431–436.
Massey SC, Miller RF. 1988. Glutamate receptors of ganglion cells in the rabbit retina: evidence for glutamate as a bipolar cell transmitter. J Physiol 405:635–655.

Mataruga A, Kremmer E, Muller F. 2007. Type 3a and type 3b OFF cone bipolar cells provide for the alternative rod pathway in the mouse retina. J Comp Neurol 502: 1123–1137.

Michel WC, Steullet P, Cate HS, Burns CJ, Zhainazarov AB, Derby CD. 1999. High-resolution functional labeling of vertebrate and invertebrate olfactory receptor neurons using agmatine, a channel-permeant cation. J Neurosci Methods 90:143–156.

Milam AH, Dacey DM, Dizhoor AM. 1993. Recoverin immunoreactivity in mammalian cone bipolar cells. Vis Neurosci 10:1–12.

Mobley AS, Michel WC, Lucero MT. 2008. Odorant responsiveness of squid olfactory receptor neurons. Anat Rec (Hoboken) 291:763–774.

Monaghan DT, Bridges RJ, Cotman CW. 1989. The excitatory amino acid receptors: their classes, pharmacology, and distinct properties in the function of the central nervous system. Annu Rev Pharmacol Toxicol 29:365–402.

Morgan IG. 1983. The organization of amacrine cell types which use different transmitters in chicken retina. Prog Brain Res 58:191–199.

Morigiwa K, Vardi N. 1999. Differential expression of ionotropic glutamate receptor subunits in the outer retina. J Comp Neurol 405:173–184.

Morkve SH, Veruki ML, Hartveit E. 2002. Functional characteristics of non-NMDA-type ionotropic glutamate receptor channels in AII amacrine cells in rat retina. J Physiol 542:147–165.

Muller F, Greferath U, Wässle H, Wisden W, Seeburg P. 1992. Glutamate receptor expression in the rat retina. Neurosci Lett 138:179–182.

Osborne NN, Larsen A, Barnett NL. 1995. Influence of excitatory amino acids and ischemia on rat retinal choline acetyltransferase-containing cells. Invest Ophthalmol Vis Sci 36: 1692–1700.

Ostermann-Latif C, Mader M, Unger JW, Bartke I, Naujoks K, Peters JH, Felgenhauer K. 1992. Characterization of mono- and polyclonal antibodies against highly purified choline acetyltransferase: a monoclonal antibody shows reactivity in human brain. J Neurochem 58:1060–1065.

Oyamada H, Takatsuji K, Senba E, Mantyh PW, Tohyama M. 1999. Postnatal development of NK1, NK2, and NK3 neurokinin receptors expression in the rat retina. Brain Res Dev Brain Res 117:59–70.

Oyster CW, Takahashi ES, Cilluffo M, Brecha NC. 1985. Morphology and distribution of tyrosine hydroxylase-like immunoreactive neurons in the cat retina. Proc Natl Acad Sci U S A 82:6335–6339.

Ozawa S, Kamiya H, Tsuzuki K. 1998. Glutamate receptors in the mammalian central nervous system. Prog Neurobiol 54: 581–618.

Pang JJ, Gao F, Wu SM. 2010. Light responses and morphology of bNOS-immunoreactive neurons in the mouse retina. J Comp Neurol 518:2456–2474.

Park CH, Kim YS, Noh HS, Cheon EW, Yang YA, Yoo JM, Choi WS, Cho GJ. 2005. Neuroprotective effect of citicoline against KA-induced neurotoxicity in the rat retina. Exp Eye Res 81:350–358.

Paternain AV, Morales M, Lerma J. 1995. Selective antagonism of AMPA receptors unmasks kainate receptor-mediated responses in hippocampal neurons. Neuron 14: 185–189.

Peng YW, Blackstone CD, Huganir RL, Yau KW. 1995. Distribution of glutamate receptor subtypes in the vertebrate retina. Neuroscience 66:483–497.

Perez MT, Caminos E. 1995. Expression of brain-derived neurotrophic factor and of its functional receptor in neonatal and adult rat retina. Neurosci Lett 183:96–9.

Picco C, Menini A. 1993. The permeability of the cGMP-activated channel to organic cations in retinal rods of the tiger salamander. J Physiol 460:741–758.

Pourcho RG. 1980. Uptake of [^{3}H]glycine and [^{3}H]GABA by amacrine cells in the cat retina. Brain Res 198:33–46.

Pourcho RG, Goebel DJ. 1983. Neuronal subpopulations in cat retina which accumulate the GABA agonist, (^{3}H)muscimol: a combined Golgi and autoradiographic study. J Comp Neurol 219:25–35.

Pow DV. 2001. Amino acids and their transporters in the retina. Neurochem Int 38:463–484.

Puller C, Haverkamp S. 2011. Bipolar cell pathways for color vision in non-primate dichromats. Vis Neurosci 28:51–60.

Puthussery T, Gayet-Primo J, Taylor WR. 2010. Localization of the calcium-binding protein secretagogin in cone bipolar cells of the mammalian retina. J Comp Neurol 518: 513–525.

Qin P, Pourcho RG. 1999. AMPA-selective glutamate receptor subunits GluR2 and GluR4 in the cat retina: an immunocytochemical study. Vis Neurosci 16:1105–1114.

Qin P, Pourcho RG. 2001. Immunocytochemical localization of kainate-selective glutamate receptor subunits GluR5, GluR6, and GluR7 in the cat retina. Brain Res 890: 211–221.

Robin LN, Kalloniatis M. 1992. Interrelationship between retinal ischaemic damage and turnover and metabolism of putative amino acid neurotransmitters, glutamate and GABA. Doc Ophthalmol 80:273–300.

Sagar SM. 1990. NADPH-diaphorase reactive neurons of the rabbit retina: differential sensitivity to excitotoxins and unusual morphologic features. J Comp Neurol 300:309–319.

Seeburg PH. 1993. The TiPS/TINS lecture: the molecular biology of mammalian glutamate receptor channels. Trends Pharmacol Sci 14:297–303.

Sommer B, Seeburg PH. 1992. Glutamate receptor channels: novel properties and new clones. Trends Pharmacol Sci 13:291–296.

Sucher NJ, Lipton SA, Dreyer EB. 1997. Molecular basis of glutamate toxicity in retinal ganglion cells. Vision Res 37: 3483–3493.

Sun D, Kalloniatis M. 2006. Mapping glutamate responses in immunocytochemically identified neurons of the mouse retina. J Comp Neurol 494:686–703.

Sun D, Rait JL, Kalloniatis M. 2003. Inner retinal neurons display differential responses to N-methyl-D-aspartate receptor activation. J Comp Neurol 465:38–56.

Sun D, Bui BV, Vingrys AJ, Kalloniatis M. 2007a. Alterations in photoreceptor-bipolar cell signaling following ischemia/reperfusion in the rat retina. J Comp Neurol 505:131–146.

Sun D, Vingrys AJ, Kalloniatis M. 2007b. Metabolic and functional profiling of the ischemic/reperfused rat retina. J Comp Neurol 505:114–130.

Sun D, Vingrys AJ, Kalloniatis M. 2007c. Metabolic and functional profiling of the normal rat retina. J Comp Neurol 505:92–113.

Thor S, Ericson J, Brannstrom T, Edlund T. 1991. The homeodomain LIM protein Isl-1 is expressed in subsets of neurons and endocrine cells in the adult rat. Neuron 7: 881–889.

Veruki ML, Morkve SH, Hartveit E. 2003. Functional properties of spontaneous EPSCs and non-NMDA receptors in rod amacrine (AII) cells in the rat retina. J Physiol 549:759–774.

Voigt T. 1986. Cholinergic amacrine cells in the rat retina. J Comp Neurol 248:19–35.

Wässle H, Grünert U, Rohrenbeck J. 1993. Immunocytochemical staining of AII-amacrine cells in the rat retina with antibodies against parvalbumin. J Comp Neurol 332: 407–420.

Yan XX, Wiechmann AF. 1997. Early expression of recoverin in a unique population of neurons in the human retina. Anat Embryol 195:51–63.

Yoshikami D. 1981. Transmitter sensitivity of neurons assayed by autoradiography. Science 212:929–930.

Young S, Rothbard J, Parker PJ. 1988. A monoclonal antibody recognising the site of limited proteolysis of protein kinase C. Inhibition of down-regulation in vivo. Eur J Biochem 173:247–252.

Yu BC, Watt CB, Lam DM, Fry KR. 1988. GABAergic ganglion cells in the rabbit retina. Brain Res 439:376–382.

Zhou C, Dacheux RF. 2004. All amacrine cells in the rabbit retina possess AMPA-, NMDA-, GABA-, and glycine-activated currents. Vis Neurosci 21:181–188.

Zhou ZJ, Marshak DW, Fain GL. 1994. Amino acid receptors of midget and parasol ganglion cells in primate retina. Proc Natl Acad Sci U S A 91:4907–4911.